

UC Berkeley

UC Berkeley Previously Published Works

Title

First measurement of $\Xi c 0$ production in pp collisions at $s = 7$ TeV

Permalink

<https://escholarship.org/uc/item/4tx7p8ps>

Authors

Acharya, S
Adamová, D
Adolfsson, J
[et al.](#)

Publication Date

2018-06-01

DOI

10.1016/j.physletb.2018.03.061

Peer reviewed



First measurement of Ξ_c^0 production in pp collisions at $\sqrt{s} = 7$ TeV

ALICE Collaboration*



ARTICLE INFO

Article history:

Received 15 December 2017
 Received in revised form 5 March 2018
 Accepted 21 March 2018
 Available online 27 March 2018
 Editor: L. Rolandi

ABSTRACT

The production of the charm-strange baryon Ξ_c^0 is measured for the first time at the LHC via its semileptonic decay into $e^+\Xi^- \nu_e$ in pp collisions at $\sqrt{s} = 7$ TeV with the ALICE detector. The transverse momentum (p_T) differential cross section multiplied by the branching ratio is presented in the interval $1 < p_T < 8$ GeV/c at mid-rapidity, $|y| < 0.5$. The transverse momentum dependence of the Ξ_c^0 baryon production relative to the D^0 meson production is compared to predictions of event generators with various tunes of the hadronisation mechanism, which are found to underestimate the measured cross-section ratio.

© 2018 The Author(s). Published by Elsevier B.V. This is an open access article under the CC BY license (<http://creativecommons.org/licenses/by/4.0/>). Funded by SCOAP³.

Quantum Chromodynamics (QCD) as the theory of the strong interaction has been a cornerstone of the Standard Model for several decades. It has been tested through measurements in e^+e^- , pp, $p\bar{p}$ and ep collisions at momentum-transfer scales where perturbative techniques are applicable [1]. In particular, measurements of charm hadrons have provided important tests of the theory because perturbative techniques are applicable down to low transverse momentum (p_T) thanks to the large mass of the charm quark compared to the QCD scale parameter ($\Lambda_{\text{QCD}} \sim 200$ MeV). The production cross sections of charm hadrons can be calculated using the factorisation approach as a convolution of three factors [2]: the parton distribution functions of the incoming protons, the hard-scattering cross section at partonic level and the fragmentation functions of charm quarks into charm hadrons. There are several state-of-the-art calculations adopting different factorisation schemes. The collinear factorisation scheme is used by calculations at next-to-leading order in α_s , such as the general-mass variable flavour number scheme (GM-VFNS) [3–5] and the fixed order with next-to-leading-log resummation (FONLL) [6,7] approaches, while the k_T factorisation scheme is employed at leading order in Refs. [8–10]. However, some of these calculations do not provide predictions for heavy-baryon production due to the lack of knowledge about the fragmentation function of charm quarks into baryonic states. Measurements of the production of charm baryons, such as Λ_c^+ and Ξ_c^0 , are essential to develop and test models of the hadronisation process.

While a variety of new charm-baryon resonances, such as Ω_c^0 [11], Ξ_{cc}^{++} [12], have recently been found, charm-hadron cross-section measurements at the Large Hadron Collider (LHC) are mainly limited to mesons [13–21], apart from a few measure-

ments of the Λ_c^+ cross section in pp and p–Pb collisions [16, 22]. In the case of Ξ_c^0 , the existing measurements are currently limited to e^+e^- collisions [23–27]. New measurements of charm-baryon production are therefore needed to provide further insights into the hadronisation processes in pp collisions. For example, interactions at the partonic level among the produced quarks and gluons, such as colour reconnection, could be stronger in pp collisions than in e^+e^- collisions, resulting in an enhanced production of baryons relative to mesons [28]. The measurements of charm-baryon production in pp collisions also serve as a reference for heavy-ion collisions, where a modification of the baryon-to-meson ratio is expected if a substantial fraction of charm quarks hadronises via recombination with other quarks from the deconfined medium created in the collision [29–33]. Measurements of charm-strange baryons, e.g. Ξ_c^0 , could also provide additional input to better understand the hadronisation mechanism of strange quarks in pp collisions because of their valence quark composition.

In this paper, we report the first measurement of the p_T -differential production cross section of Ξ_c^0 multiplied by the branching ratio (BR) into the semileptonic decay mode, $\Xi_c^0 \rightarrow e^+\Xi^- \nu_e$, and its ratio to the measured production cross section of D^0 mesons [21] as a function of p_T , up to 8 GeV/c. The absolute branching ratio of this Ξ_c^0 decay is currently unknown [34]. Using a data sample of pp collisions at $\sqrt{s} = 7$ TeV recorded with the ALICE detector in 2010, the measurement is performed by analysing $e^+\Xi^-$ pairs formed by combining positrons and Ξ^- baryons reconstructed with the detectors of the ALICE central barrel, covering the pseudorapidity interval $|\eta| < 0.9$. The missing momentum of the neutrino is corrected using unfolding techniques. Charge conjugate modes are implied everywhere, unless otherwise stated. Only the sub-detectors relevant for this data analysis are described below. A more complete and detailed description of the ALICE detector and its performance can be found in Refs. [35,36].

* E-mail address: alice-publications@cern.ch.

The detectors used in this analysis include the Inner Tracking System (ITS), the Time Projection Chamber (TPC) and the Time-Of-Flight detector (TOF). These detectors are located in a large solenoid magnet producing a magnetic field of 0.5 T parallel to the LHC beam axis. The ITS consists of six cylindrical layers of silicon detectors, placed at radial distances ranging from 3.9 cm to 43 cm from the nominal beam axis and covering the full azimuth. The two innermost layers consist of Silicon Pixel Detectors (SPD), the two intermediate layers of Silicon Drift Detectors (SDD) and the two outermost layers of Silicon Strip Detectors (SSD). The total material budget of the ITS is on average 7.7% of a radiation length, for particles with $\eta = 0$ [37]. The ITS spatial resolution enables the measurement of the distance of closest approach (d_0) of tracks to the primary vertex with a resolution better than 75 μm in the transverse plane for $p_T > 1$ GeV/c in pp collisions [38]. The TPC is a cylindrical gaseous detector with a volume of about 90 m³. The TPC provides track reconstruction with up to 159 space points at radial distances from the beam axis ranging between 85 cm and 247 cm, within the full azimuth. The TPC cluster-position resolution is about 500 μm along the beam direction and in the transverse direction for tracks with $\eta = 0$ [39]. The TPC also provides particle identification capabilities via the measurement of the specific ionisation energy loss, dE/dx , with a resolution of approximately 5.2% in pp collisions [36]. The TOF detector consists of multi-gap resistive plate chambers placed at a radial distance of 3.7 m from the beam axis and also covers the full azimuth. The TOF detector, with a timing resolution of about 80 ps, measures the time-of-flight of particles relative to the time of the collision, which is determined by the arrival time of the particles at the TOF detector and by the T0 detector, an array of Cherenkov counters placed at +370 cm and -70 cm from the nominal interaction point along the beam axis [40].

The analysed data sample consists of pp collisions at $\sqrt{s} = 7$ TeV recorded during the 2010 LHC data taking period with a minimum bias trigger that requires at least one hit in either the SPD or the V0 detectors. The two layers of the SPD detector cover $|\eta| < 2.0$. The two V0 detectors, each comprising 32 scintillator tiles, are installed on both sides of the interaction point and cover $-3.7 < \eta < -1.7$ and $2.8 < \eta < 5.1$. The trigger condition captures 87% of the pp inelastic cross section [41]. The collision vertex is reconstructed with an efficiency of 88% and only events with a reconstructed vertex within 10 cm from the nominal interaction point along the beam direction are used in this analysis. Pile-up events are identified by searching for a second interaction vertex, reconstructed with at least three SPD tracklets (that are two-point track segments connecting hits in the two SPD layers) pointing to a common vertex, which is separated from the first vertex by at least 8 mm. After the selections, the analysed sample corresponds to an integrated luminosity $L_{\text{int}} = 5.9 \pm 0.2 \text{ nb}^{-1}$.

The Ξ_c^0 candidates are defined from $e^+\Xi^-$ pairs by combining a track originating from the primary vertex (denoted by “electron track” in the following) and a reconstructed Ξ^- baryon. Electron tracks satisfying $|\eta| < 0.8$ and $p_T > 0.5$ GeV/c are required to have at least 100 associated clusters in the TPC (out of which at least 80 are used for the calculation of the dE/dx signal), a χ^2 normalised to the number of TPC clusters smaller than 4 and at least 4 hits in the ITS. It is also required that the electron track has associated hits in the two innermost layers of the ITS, in order to reject electrons from photon conversions occurring in the detector material outside the innermost SPD layer [13]. Electrons are identified using the dE/dx measurement in the TPC and the time-of-flight measurement of the TOF detector. In both cases, the selection is applied on the n_{σ}^{TPC} and n_{σ}^{TOF} variables defined as the difference between the measured dE/dx or time-of-flight values and the one expected for electrons, divided by the corresponding detector res-

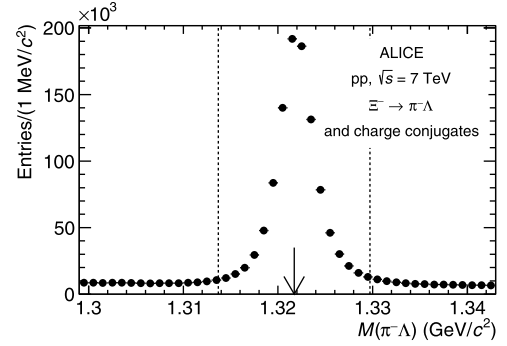


Fig. 1. Invariant-mass distribution of $\Xi^- \rightarrow \pi^- \Lambda$ (and charge conjugate) candidates integrated over p_T . The arrow indicates the world average Ξ^- mass from Ref. [34] and the dashed lines indicate the selected interval for the Ξ^- candidates.

olution. The following selection criteria are applied: $|n_{\sigma}^{\text{TOF}}| < 3$ and $-3.9 + 1.2p_T - 0.094p_T^2 < n_{\sigma}^{\text{TPC}}(p_T) < 3$. The p_T -dependent lower limit on n_{σ}^{TPC} was optimised to reject hadrons. Thus, an electron purity of 98% is achieved over the whole p_T range.

The background from “photonic” electrons (originating from Dalitz decays of neutral mesons and photon conversions in the detector material) remaining in the electron sample are identified using a technique based on the invariant mass of e^+e^- pairs [42]. The electron tracks are paired with opposite-sign tracks from the same event passing loose selection criteria ($|n_{\sigma}^{\text{TPC}}| < 5$ without TOF requirement) and are identified as photonic electrons if there is at least one pair with an invariant mass smaller than 50 MeV/c². Setting such loose electron identification criteria is meant to increase the efficiency of finding the partners. This improves the signal-to-background ratio for Ξ_c^0 by about 50%, while the fraction of the signal lost due to misidentifications is less than 2%.

The Ξ^- baryons are reconstructed from the decay chain $\Xi^- \rightarrow \pi^- \Lambda$, followed by $\Lambda \rightarrow p\pi^-$. Tracks used to define Ξ^- candidates are required to have at least 80 clusters in the TPC and a dE/dx signal in the TPC consistent with the expected values for protons (pions) within 4σ . The Ξ^- and Λ baryons have long lifetimes ($c\tau$ of about 4.91 cm and 7.89 cm, respectively [34]), and thus they can be identified using their characteristic cascade-like or V-shaped decay topologies [43–45]. Pions originating directly from Ξ^- decays are selected by requiring $d_0 > 0.02$ cm; protons and pions originating from Λ decays are required to have $d_0 > 0.07$ cm. The d_0 of the Λ trajectory to the primary vertex is required to be larger than 0.03 cm, while its cosine of the pointing angle, which is the angle between the reconstructed Λ momentum and the line connecting the Λ and Ξ^- decay vertices, is required to be larger than 0.98. The distances of the Ξ^- and Λ decay vertices from the beam line are required to be larger than 0.4 and 2.7 cm, respectively. These selection criteria are tuned to reduce the background, while keeping a high efficiency for the signal. Fig. 1 shows the Ξ^- peak in the $\pi^- \Lambda$ invariant-mass distribution integrated over p_T . Only Ξ^- candidates with invariant masses within 8 MeV/c² from the Ξ^- mass (1321.71 ± 0.07 MeV/c² [34]) indicated by an arrow in Fig. 1 are kept for further analysis. In this interval, the signal-to-background ratio is about 8.

The $e^+\Xi^-$ pairs are formed from selected positrons and Ξ^- candidates. Only pairs with an opening angle smaller than 90 degrees are used for the analysis. The background in the $e^+\Xi^-$ pair distribution is estimated by exploiting the fact that Ξ_c^0 baryons decay into $e^+\Xi^- \nu_e$ (right-sign, RS), but not into $e^-\Xi^- \bar{\nu}_e$ (wrong-sign, WS), while most of the background sources contribute equally to RS and WS pairs. The yield of WS pairs is therefore used to estimate the background and is subtracted from the yield of RS pairs to obtain the Ξ_c^0 raw yield. The procedure is verified with

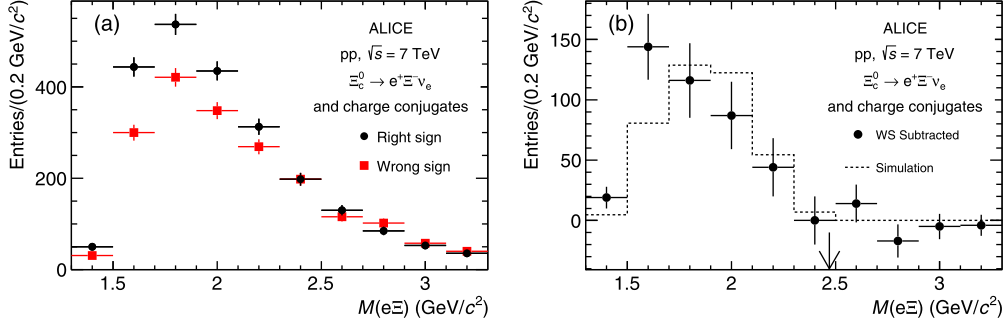


Fig. 2. (a) Invariant-mass distributions of right-sign and wrong-sign (and charge conjugate) pairs integrated over the whole p_T interval. (b) Invariant-mass distribution of Ξ_c^0 candidates obtained by subtracting the wrong-sign pair yield from the right-sign one compared with the signal distribution from the simulation, which is normalised to the measured RS–WS yield. The arrow indicates the Ξ_c^0 mass [34].

PYTHIA 6.4.21 [46] simulations using the Perugia-0 tune [47] and the GEANT3 transport code [48], including a realistic description of the detector response and alignment during the data taking period. A similar procedure was adopted by the ARGUS and CLEO collaborations studying e^+e^- collisions [24,25].

Fig. 2(a) shows the invariant-mass distributions of RS and WS pairs, integrated over the whole p_T interval. The invariant-mass distribution of Ξ_c^0 candidates obtained by subtracting the WS pair yield from the RS one is shown in Fig. 2(b) together with the signal distribution from the simulation, which is normalised to the measured RS–WS yield. The shapes of the two distributions are found to be consistent with each other. Due to the missing momentum of the neutrino, the invariant-mass distribution of the $e^+\Xi^-$ pair does not peak at the Ξ_c^0 mass ($2470.85^{+0.28}_{-0.40}$ MeV/ c^2 [34]) indicated by an arrow in Fig. 2(b). The invariant mass of $e^+\Xi^-$ pairs from Ξ_c^0 decays is bounded by the Ξ_c^0 mass due to the missing momentum of the neutrino. Thus only $e^+\Xi^-$ pairs satisfying $m_{e\Xi} < 2.5$ GeV/ c^2 are selected for further analysis.

In order to obtain the p_T -differential production cross section of Ξ_c^0 baryons, the background-subtracted (WS-subtracted) yield needs to be corrected for: the signal loss due to misidentification of photonic electrons, the Ξ_b contribution in the WS pairs, the missing neutrino momentum, the detector acceptance and the track-reconstruction and the candidate-selection efficiencies. No correction is applied for possible differences in the acceptance of RS and WS pairs, which are found to be negligible for the current analysis based on a study with the mixed-event technique (i.e. by pairing electrons and Ξ^- from different events).

The first correction accounts for the signal loss caused by the misidentification of photonic electrons. The misidentification occurs when electrons from Ξ_c^0 decays accidentally have opposite-sign partners giving rise to a very small invariant mass of the e^+e^- pair. The misidentification probability is estimated to be less than 2% by applying the tagging algorithm to e^+e^+ and e^-e^- pairs. The correction is applied as a function of the p_T of the $e^+\Xi^-$ pair.

The second correction accounts for the overestimation of the background caused by $\Xi_b \rightarrow e^-\Xi^-\bar{\nu}_e X$ decays, which produce WS pairs. Since the branching ratio of Ξ_b into $e^-\Xi^-\bar{\nu}_e X$ and the Ξ_b cross section in pp collisions at LHC energies have not been measured yet, two assumptions are made to estimate this contribution. First, the shape of the transverse momentum distribution of the Ξ_b baryon is assumed to be the same as that of Λ_b^0 , which was measured for $p_T > 10$ GeV/ c and $|y| < 2$ by the CMS collaboration [49]. This measurement is extrapolated to $p_T = 0$ using the Tsallis function,

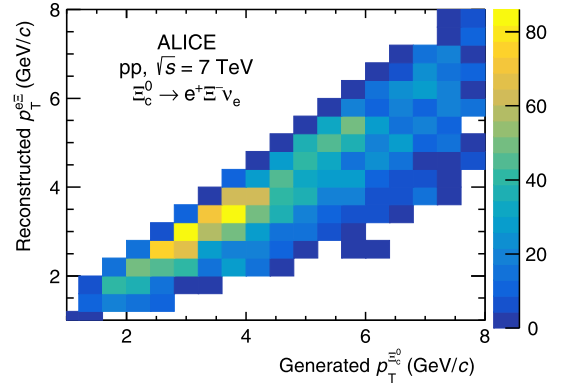


Fig. 3. Correlation between the generated Ξ_c^0 -baryon p_T and the reconstructed $e^+\Xi^-$ pair p_T , obtained from the simulation based on PYTHIA 6 described in the text. (For interpretation of the colours in the figure(s), the reader is referred to the web version of this article.)

$$Cp_T \left[1 + \frac{\sqrt{p_T^2 + m^2} - m}{nT} \right] \quad (1)$$

whose parameters were also determined by the CMS collaboration by fitting the measured distribution. The fit parameters are consistent with those determined by the LHCb collaboration for the measurement of Λ_b^0 down to $p_T = 0$ at forward rapidity ($2 < y < 4.5$) [50]. The second hypothesis is made for the total yield of $\Xi_b \rightarrow e^-\Xi^-\bar{\nu}_e X$, which is determined by using the measurements of $\text{BR}(b \rightarrow \Xi_b) \cdot \text{BR}(\Xi_b \rightarrow \Xi^- l^+ \bar{\nu} X)$ [51] and $\text{BR}(b \rightarrow \Lambda_b^0) \cdot \text{BR}(\Lambda_b^0 \rightarrow \Lambda l^+ \bar{\nu} X)$ [52] in e^+e^- collisions and by assuming that the fraction of beauty quarks that hadronise into Λ_b^0 and Ξ_b baryons are the same as those in e^+e^- collisions. This assumption is supported by B-meson measurements, which show that the yield of B_s^0 mesons relative to non-strange B mesons is consistent in e^+e^- and $p\bar{p}$ collisions [53]. The Ξ_b distribution obtained with these assumptions is further processed to take into account the detector acceptance, efficiency and the momentum carried by non-reconstructed decay particles. This is done with the PYTHIA 6 simulation using GEANT3 for particle transport through the detector. The correction increases with p_T and reaches 2% at the highest p_T interval.

The transverse momentum distribution of $e^+\Xi^-$ pairs is corrected for the missing momentum of the neutrino using unfolding techniques. The response matrix to correct for the missing neutrino momentum is generated based on the correlation between the p_T of the Ξ_c^0 baryon and that of the reconstructed $e^+\Xi^-$ pair, which is obtained from the simulation described above and is shown in Fig. 3. The response matrix includes both the decay kinematics and

Table 1

Summary of systematic uncertainties on the p_T -differential cross section of $\Xi_c^0 \rightarrow e^+ \Xi^- \nu_e$ for 5 p_T intervals. The uncertainty on the missing neutrino momentum is denoted as p_T^ν in the table.

Source	Relative systematic uncertainty (%) in the measured p_T intervals (GeV/c)				
	1–2	2–3.2	3.2–4.4	4.4–6	6–8
Raw yield	5	5	5	5	5
$(A \times \varepsilon)$	30	22	16	13	14
p_T^ν	29	8	6	7	10
Normalisation	3.5				

the instrumental effects, such as energy loss and bremsstrahlung in the detector material. The response matrix needs to be determined using a realistic Ξ_c^0 -baryon p_T distribution. However, the distribution is not known *a priori*. Therefore, the response matrix is prepared in two steps. In the first step, the response matrix is obtained with the p_T distribution generated with PYTHIA 6. The resulting Ξ_c^0 momentum distribution is used to produce the response matrix for the second iteration. The unfolding is performed with the RooUnfold [54] implementation of the Bayesian unfolding technique [55], which is an iterative method based on Bayes' theorem. Convergence of the Bayesian method is achieved after three iterations.

The p_T -differential production cross section of Ξ_c^0 baryons multiplied by the branching ratio into the considered semileptonic decay channel is calculated from the yields obtained by the unfolding approach as follows:

$$\text{BR} \cdot \frac{d^2\sigma^{\Xi_c^0}}{dp_T dy} = \frac{N_{\Xi_c^0}}{2 \cdot \Delta p_T \Delta y \cdot (A \times \varepsilon) \cdot L_{\text{int}} \cdot \text{BR}_{\Xi_c^-}}, \quad (2)$$

where $N_{\Xi_c^0}$ is the yield in a given p_T interval with width Δp_T . The yield is divided by the integrated luminosity L_{int} of the analysed sample and by the product of the branching ratios of the decays $\Xi_c^- \rightarrow \pi^- \Lambda$ ($99.887 \pm 0.035\%$ [34]) and $\Lambda \rightarrow p\pi^-$ ($63.9 \pm 0.5\%$ [34]), which is indicated as $\text{BR}_{\Xi_c^-}$. The factor 1/2 is needed because the cross section is computed for the average of Ξ_c^0 and Ξ_c^+ , while the raw yield includes both contributions. The factor $(A \times \varepsilon)$ is the product of the geometrical acceptance (A) and the reconstruction and selection efficiency (ε) for $\Xi_c^0 \rightarrow e^+ \Xi^- \nu_e$ decays determined for Ξ_c^0 generated in $|y| < 0.8$. Finally, the yield is normalised to one unit of rapidity by dividing it by $\Delta y = 1.6$ under the assumption that the rapidity distribution of Ξ_c^0 is uniform in the range $|y| < 0.8$. This assumption is verified with an accuracy of 1% using PYTHIA 6. Note that the flatness of the rapidity distribution in $|y| < 0.8$ is also relevant for the comparison to the D^0 meson cross section, which was determined in $|y| < 0.5$ [21].

The acceptance and the efficiency are calculated from the simulations with an additional correction to take into account the fact that the elastic cross section of anti-protons is not accurate in GEANT3 [56]. The correction is calculated using the GEANT4 transport code [57], which has a more accurate description of the cross section, and found to be less than 2%. Since the acceptance and the efficiency depend on the Ξ_c^0 -baryon p_T , the Ξ_c^0 should be generated with a realistic momentum distribution. This was obtained via a two-step procedure similar to that used for the response matrix. Fig. 4 shows the product of the geometrical acceptance and the reconstruction and selection efficiency ($A \times \varepsilon$) of Ξ_c^0 as a function of p_T .

The systematic uncertainty on the Ξ_c^0 cross section has different contributions, which are the uncertainties on the raw yield (owing to the procedure of background estimation), on the $(A \times \varepsilon)$ factor (due to imperfections in the simulated samples), on the correction of the missing neutrino momentum (related to the unfolding procedure) and on the normalisation. Table 1 summarises

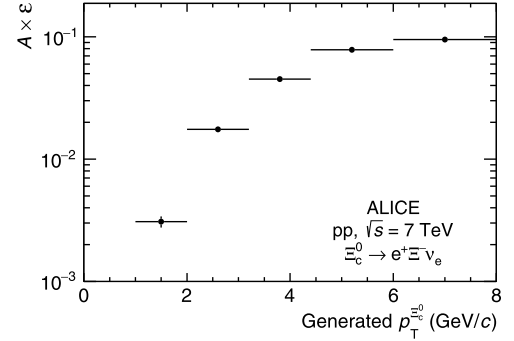


Fig. 4. Product of acceptance and efficiency ($A \times \varepsilon$) of Ξ_c^0 baryons generated in $|y| < 0.8$ decaying into $e^+ \Xi^- \nu_e$ as a function of p_T , determined from simulations PYTHIA 6 (see text).

the estimated systematic uncertainties, reporting their values in all the p_T intervals. The total systematic uncertainty is determined by adding the individual contributions in quadrature in each p_T interval.

The systematic uncertainty on the raw yield includes the uncertainties due to the WS subtraction procedure and to the estimation of the Ξ_b contribution. In the WS subtraction procedure described above, it was assumed that all the background sources contribute equally to RS and WS pairs. This is true as long as the background comprises uncorrelated pairs of electrons and Ξ^- . A systematic uncertainty of 4% on the Ξ_c^0 signal yield due to possible differences between RS and WS is estimated from simulations with the PYTHIA 6 event generator by checking the remaining contamination of background pairs in the RS yield after the subtraction of the WS pairs. The WS subtraction could also be affected by the amount of hadron contamination in the electron sample and the signal-to-background ratio of the Ξ_c^0 signal. This effect is studied by repeating the analysis with different electron identification criteria. The results obtained with these modified criteria are found to be consistent with the ones from the default selections and therefore no systematic uncertainty is assigned. The systematic uncertainty due to the Ξ_b contribution to the WS pairs is estimated by varying the Ξ_b momentum distribution within the quoted uncertainty of about 50% on the cross section of Λ_b^0 in pp collisions [49] and the quoted uncertainty of about 50% on the ratio of the fragmentation fractions of beauty quarks into Λ_b^0 and Ξ_b in e^+e^- collisions [51, 52]. The effect on the final results is found to be about 1% because the contribution from Ξ_b is small. These systematic uncertainties add up to a total uncertainty of 5% for the raw yield extraction.

The systematic uncertainties arising from the reconstruction and selection efficiencies are estimated by repeating the analysis with different selection criteria for electrons, Ξ^- and $e^+ \Xi^-$ pairs and by comparing the corrected yields. Due to the statistical limitations of the Ξ_c^0 sample, the electron efficiencies are studied via variations of the track-quality criteria and of the n_σ values for the electron identification with TPC and TOF in the $\Lambda_c^+ \rightarrow e^+ \Lambda \nu_e$ decays, which are analysed with the same procedure and have higher statistical significance. The RMS of the deviations of the corrected

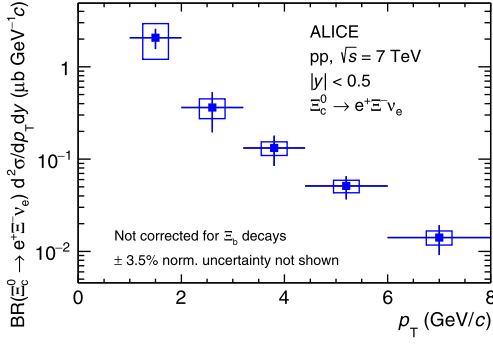


Fig. 5. Inclusive Ξ_c^0 -baryon p_T -differential production cross section multiplied by the branching ratio into $e^+ \Xi^- \nu_e$, as a function of p_T for $|y| < 0.5$, in pp collisions at $\sqrt{s} = 7$ TeV. The error bars and boxes represent the statistical and systematic uncertainties, respectively. The contribution from Ξ_b decays is not subtracted.

yields relative to the value obtained with the standard selection criteria, which amounts to 4% and 3%, is then assigned as a systematic uncertainty on the reconstruction and selection efficiency. Similarly, a systematic uncertainty of 1% on both the Ξ^- reconstruction and selection efficiency is estimated from the RMS deviation of the inclusive Ξ^- corrected yield against variations of the criteria applied to select the Ξ^- decay tracks and its cascade decay topology. In addition, a systematic uncertainty of 4% on the Ξ^- efficiency due to possible imperfections in the description of the detector material in the simulations [44] is considered and summed in quadrature with that estimated from the variation of the selection criteria. The uncertainties on the electron and Ξ^- track-quality criteria are considered as correlated and combined linearly. The uncertainty on the $e^+ \Xi^-$ pair selection efficiency is estimated by varying the selection criteria on the opening angle and the invariant mass of the pair and a systematic uncertainty of 3–27% is assigned depending on p_T . Finally, a systematic uncertainty may also arise from an imperfect description of the acceptance of $e^+ \Xi^-$ pairs in the simulation. It is estimated to be 11% by comparing the azimuthal distributions of inclusive electrons and Ξ^- baryons in the data and in the simulation. The uncertainty on the $e^+ \Xi^-$ pair acceptance is summed in quadrature with that on the electron and Ξ^- selection efficiencies, resulting in a systematic uncertainty on the $(A \times \varepsilon)$ correction factor ranging from 13% to 30% depending on p_T .

The systematic uncertainty on the missing neutrino momentum correction with the unfolding procedure is evaluated by varying the prior distribution to the Bayesian unfolding and by using different unfolding techniques, such as the χ^2 minimisation method [58, 59] and the Singular Value Decomposition (SVD) method [60]. The RMS deviation of the results, ranging between 4% and 29% depending on p_T , is assigned as a systematic uncertainty. A systematic uncertainty of 3% is also assigned due to the imperfect knowledge of the Ξ_c^0 -baryon p_T distributions used as input for the efficiency calculation and the unfolding procedure from the simulation. It is estimated from the difference induced in the result by adding an additional step in the iterative procedure described above to obtain the input p_T distributions. These systematic uncertainties add up to an uncertainty ranging between 6% and 29% depending on p_T .

Finally, the results have a 3.5% normalisation systematic uncertainty arising from the uncertainty in the determination of the minimum-bias trigger cross section in pp collisions at $\sqrt{s} = 7$ TeV [41].

The p_T -differential cross section of Ξ_c^0 baryons multiplied by the branching ratio into $e^+ \Xi^- \nu_e$ is shown in Fig. 5 for the p_T interval $1 < p_T < 8$ GeV/c at mid-rapidity, $|y| < 0.5$. The error bars and boxes represent the statistical and systematic uncertainties, respectively. The feed down contribution from Ξ_b , e.g.

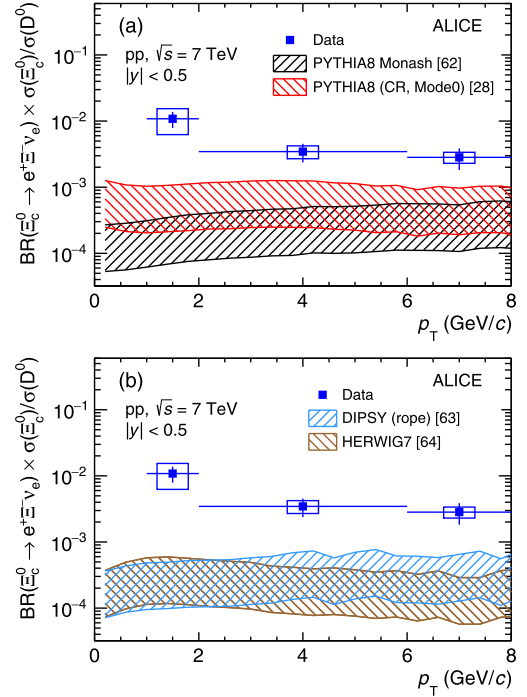


Fig. 6. Ratio of the p_T -differential cross sections of Ξ_c^0 baryons (multiplied by the branching ratio into $e^+ \Xi^- \nu_e$) and D^0 mesons [21] as a function of p_T for $|y| < 0.5$, in pp collisions at $\sqrt{s} = 7$ TeV. The error bars and boxes represent the statistical and systematic uncertainties, respectively. Predictions from theoretical models, (a) PYTHIA 8 with different tunes [28,62]. (b) DIPSY [63] and HERWIG 7 [64], are shown as shaded bands representing the range of the currently available theoretical predictions for the branching ratio of the considered Ξ_c^0 decay mode.

$\Xi_b^- \rightarrow \Xi_c^0 \pi^-$ [61], is not subtracted due to the lack of knowledge of the absolute branching ratios of $\Xi_b \rightarrow \Xi_c^0 + X$.

The ratio of the p_T -differential cross section of Ξ_c^0 baryons to that of D^0 mesons [21] is shown in Fig. 6. The p_T intervals of the cross-section measurements are combined to have the same p_T bin boundaries for Ξ_c^0 and D^0 . The systematic uncertainty in a merged p_T interval is defined by propagating the yield extraction uncertainties of the D^0 measurement as uncorrelated among p_T intervals and all the other uncertainties of the D^0 and Ξ_c^0 measurements as correlated. The systematic uncertainty on the Ξ_c^0/D^0 ratio is calculated treating all the uncertainties on the Ξ_c^0 and D^0 cross sections as uncorrelated, except for the normalisation uncertainty that cancels out in the ratio. The ratio integrated in the transverse momentum interval $1 < p_T < 8$ GeV/c is found to be $(7.0 \pm 1.5(\text{stat}) \pm 2.6(\text{syst})) \times 10^{-3}$.

In Fig. 6(a), the measured transverse momentum dependence of the Ξ_c^0/D^0 ratio is compared with predictions from the PYTHIA 8.211 event generator [46,65]. PYTHIA 8 uses $2 \rightarrow 2$ processes followed by a leading-logarithmic p_T -ordered parton shower for the charm quark pair production and the hadronisation is treated with the Lund string model [66]. The figure shows the results obtained with different tunes of hadronisation: the Monash 2013 tune [62] and the Mode 0 tune from [28]. The latter is based on a model for the hadronisation of multi-parton systems, which includes string formation beyond the leading-colour approximation and is implemented in PYTHIA 8 with specific tuning of the colour reconnection parameters. As compared to the Monash 2013 tune, this model provides a better description of the measured baryon-to-meson ratios in the light-flavour sector. Two other tunes (Mode 2 and Mode 3) provided in Ref. [28] give similar Ξ_c^0/D^0 ratios as Mode 0. In Fig. 6(b), the measured ratio is also compared to other models implementing different hadronisation mechanisms: DIPSY [63]

with the rope hadronisation [67] and HERWIG 7.0.4 [64] with the cluster hadronisation [68]. To compare the data with these models, theoretical calculations of the branching ratio, which range between 0.83% and 4.2% [69–71], are used. This range defines the width of the bands shown for the model calculations represented in Fig. 6. Although the predictions of the Mode 0 tune of PYTHIA 8 are the closest to the data compared to the other models, all calculations underestimate the measured ratio significantly. Thus, this new measurement can provide an important constraint to the models of charm quark hadronisation in pp collisions, once a measurement of the absolute branching ratio of the Ξ_c^0 will become available.

In summary, we reported on the first LHC measurement of the inclusive p_T -differential production cross section of the charm-strange baryon Ξ_c^0 multiplied by the branching ratio into $e^+ \Xi^- \nu_e$ in pp collisions at $\sqrt{s} = 7$ TeV. The ratio of this measurement integrated over $1 < p_T < 8$ GeV/c to the production cross section of the D^0 meson integrated over the same p_T interval was found to be $(7.0 \pm 1.5(\text{stat}) \pm 2.6(\text{syst})) \times 10^{-3}$. Several event generators with various models and tunes for the hadronisation mechanism underestimate the measured ratio.

Acknowledgements

The ALICE Collaboration would like to thank all its engineers and technicians for their invaluable contributions to the construction of the experiment and the CERN accelerator teams for the outstanding performance of the LHC complex. The ALICE Collaboration gratefully acknowledges the resources and support provided by all Grid centres and the Worldwide LHC Computing Grid (WLCG) collaboration. The ALICE Collaboration acknowledges the following funding agencies for their support in building and running the ALICE detector: A.I. Alikhanyan National Science Laboratory (Yerevan Physics Institute) Foundation (ANSL), State Committee of Science and World Federation of Scientists (WFS), Armenia; Austrian Academy of Sciences and Nationalstiftung für Forschung, Technologie und Entwicklung, Austria; Ministry of Communications and High Technologies, National Nuclear Research Center, Azerbaijan; Conselho Nacional de Desenvolvimento Científico e Tecnológico (CNPq), Universidade Federal do Rio Grande do Sul (UFRGS), Financiadora de Estudos e Projetos (Finep) and Fundação de Amparo à Pesquisa do Estado de São Paulo (FAPESP), Brazil; Ministry of Science & Technology of China (MSTC), National Natural Science Foundation of China (NSFC) and Ministry of Education of China (MOEC), China; Ministry of Science, Education and Sports and Croatian Science Foundation, Croatia; Ministry of Education, Youth and Sports of the Czech Republic, Czech Republic; The Danish Council for Independent Research—Natural Sciences, the Carlsberg Foundation and Danish National Research Foundation (DNRF), Denmark; Helsinki Institute of Physics (HIP), Finland; Commissariat à l'Énergie Atomique (CEA) and Institut National de Physique Nucléaire et de Physique des Particules (IN2P3) and Centre National de la Recherche Scientifique (CNRS), France; Bundesministerium für Bildung, Wissenschaft, Forschung und Technologie (BMBF) and GSI Helmholtzzentrum für Schwerionenforschung GmbH, Germany; General Secretariat for Research and Technology, Ministry of Education, Research and Religions, Greece; National Research, Development and Innovation Office, Hungary; Department of Atomic Energy, Government of India (DAE), Department of Science and Technology, Government of India (DST), University Grants Commission, Government of India (UGC) and Council of Scientific and Industrial Research (CSIR), India; Indonesian Institute of Science, Indonesia; Centro Fermi – Museo Storico della Fisica e Centro Studi e Ricerche Enrico Fermi and Istituto Nazionale di Fisica Nucleare (INFN), Italy; Institute for Innovative Science and Tech-

nology, Nagasaki Institute of Applied Science (IIST), Japan Society for the Promotion of Science (JSPS) KAKENHI and Japanese Ministry of Education, Culture, Sports, Science and Technology (MEXT), Japan; Consejo Nacional de Ciencia (CONACYT) y Tecnología, through Fondo de Cooperación Internacional en Ciencia y Tecnología (FONCICYT) and Dirección General de Asuntos del Personal Académico (DGAPA), Mexico; Nederlandse Organisatie voor Wetenschappelijk Onderzoek (NWO), Netherlands; The Research Council of Norway, Norway; Commission on Science and Technology for Sustainable Development in the South (COMSATS), Pakistan; Pontificia Universidad Católica del Perú, Peru; Ministry of Education and Higher Education and National Science Centre, Poland; Korea Institute of Science and Technology Information and National Research Foundation of Korea (NRF), Republic of Korea; Ministry of Education and Scientific Research, Institute of Atomic Physics and Romanian National Agency for Science, Technology and Innovation, Romania; Joint Institute for Nuclear Research (JINR), Ministry of Education and Science of the Russian Federation and National Research Centre Kurchatov Institute, Russia; Ministry of Education, Science, Research and Sport of the Slovak Republic, Slovakia; National Research Foundation of South Africa, South Africa; Centro de Aplicaciones Tecnológicas y Desarrollo Nuclear (CEADEN), Cubaenergía, Cuba and Centro de Investigaciones Energéticas, Medioambientales y Tecnológicas (CIEMAT), Spain; Swedish Research Council (VR) and Knut & Alice Wallenberg Foundation (KAW), Sweden; European Organization for Nuclear Research, Switzerland; National Science and Technology Development Agency (NSDTA), Suranaree University of Technology (SUT) and Office of the Higher Education Commission under NRU project of Thailand, Thailand; Turkish Atomic Energy Agency (TAEK), Turkey; National Academy of Sciences of Ukraine, Ukraine; Science and Technology Facilities Council (STFC), United Kingdom; National Science Foundation of the United States (NSF) and United States Department of Energy, Office of Nuclear Physics (DOE NP), United States.

References

- [1] R.K. Ellis, W.J. Stirling, B.R. Webber, *QCD and Collider Physics*, Cambridge University Press, 1996.
- [2] J.C. Collins, D.E. Soper, G.F. Sterman, Heavy particle production in high-energy hadron collisions, *Nucl. Phys. B* 263 (1986) 37.
- [3] B.A. Kniehl, G. Kramer, I. Schienbein, H. Spiesberger, Inclusive $D^{*\pm}$ production in p anti-p collisions with massive charm quarks, *Phys. Rev. D* 71 (2005) 014018, arXiv:hep-ph/0410289.
- [4] B.A. Kniehl, G. Kramer, I. Schienbein, H. Spiesberger, Collinear subtractions in hadroproduction of heavy quarks, *Eur. Phys. J. C* 41 (2005) 199, arXiv:hep-ph/0502194.
- [5] B.A. Kniehl, G. Kramer, I. Schienbein, H. Spiesberger, Inclusive charmed-meson production at the CERN LHC, *Eur. Phys. J. C* 72 (2012) 2082, arXiv:1202.0439 [hep-ph].
- [6] M. Cacciari, M. Greco, P. Nason, The p_T spectrum in heavy flavor hadroproduction, *J. High Energy Phys.* 05 (1998) 007, arXiv:hep-ph/9803400.
- [7] M. Cacciari, S. Frixione, N. Houdeau, M.L. Mangano, P. Nason, G. Ridolfi, Theoretical predictions for charm and bottom production at the LHC, *J. High Energy Phys.* 10 (2012) 137, arXiv:1205.6344 [hep-ph].
- [8] S. Catani, M. Ciafaloni, F. Hautmann, High-energy factorization and small x heavy flavor production, *Nucl. Phys. B* 366 (1991) 135.
- [9] M. Luszczak, R. Maciula, A. Szczurek, Nonphotonic electrons at RHIC within k_T -factorization approach and with experimental semileptonic decay functions, *Phys. Rev. D* 79 (2009) 034009, arXiv:0807.5044 [hep-ph].
- [10] R. Maciula, A. Szczurek, Open charm production at the LHC – k_T -factorization approach, *Phys. Rev. D* 87 (2013) 094022, arXiv:1301.3033 [hep-ph].
- [11] LHCb Collaboration, R. Aaij, et al., Observation of five new narrow Ω_c^0 states decaying to $\Xi_c^+ K^-$, *Phys. Rev. Lett.* 118 (18) (2017) 182001, arXiv:1703.04639 [hep-ex].
- [12] LHCb Collaboration, R. Aaij, et al., Observation of the doubly charmed baryon Ξ_{cc}^{++} , arXiv:1707.01621 [hep-ex].
- [13] ALICE Collaboration, B. Abelev, et al., Measurement of electrons from semileptonic heavy-flavour hadron decays in pp collisions at $\sqrt{s} = 7$ TeV, *Phys. Rev. D* 86 (2012) 112007, arXiv:1205.5423 [hep-ex].

- [14] ALICE Collaboration, B. Abelev, et al., Production of muons from heavy flavour decays at forward rapidity in pp and Pb–Pb collisions at $\sqrt{s_{NN}} = 2.76$ TeV, Phys. Rev. Lett. 109 (2012) 112301, arXiv:1205.6443 [hep-ex].
- [15] ALICE Collaboration, B. Abelev, et al., Heavy flavour decay muon production at forward rapidity in proton–proton collisions at $\sqrt{s} = 7$ TeV, Phys. Lett. B 708 (2012) 265–275, arXiv:1201.3791 [hep-ex].
- [16] LHCb Collaboration, R. Aaij, et al., Prompt charm production in pp collisions at $\sqrt{s} = 7$ TeV, Nucl. Phys. B 871 (2013) 1, arXiv:1302.2864 [hep-ex].
- [17] ALICE Collaboration, B. Abelev, et al., Measurement of electrons from semileptonic heavy-flavor hadron decays in pp collisions at $\sqrt{s} = 2.76$ TeV, Phys. Rev. D 91 (2015) 012001, arXiv:1405.4117 [nucl-ex].
- [18] LHCb Collaboration, R. Aaij, et al., Measurements of prompt charm production cross-sections in pp collisions at $\sqrt{s} = 13$ TeV, J. High Energy Phys. 03 (2016) 159, arXiv:1510.01707 [hep-ex]; J. High Energy Phys. 05 (2017) 074 (Erratum).
- [19] ATLAS Collaboration, G. Aad, et al., Measurement of $D^{*\pm}$, D^{\pm} and D_s^{\pm} meson production cross sections in pp collisions at $\sqrt{s} = 7$ TeV with the ATLAS detector, Nucl. Phys. B 907 (2016) 717, arXiv:1512.02913 [hep-ex].
- [20] LHCb Collaboration, R. Aaij, et al., Measurements of prompt charm production cross-sections in pp collisions at $\sqrt{s} = 5$ TeV, arXiv:1610.02230 [hep-ex].
- [21] ALICE Collaboration, S. Acharya, et al., Measurement of D-meson production at mid-rapidity in pp collisions at $\sqrt{s} = 7$ TeV, arXiv:1702.00766 [hep-ex].
- [22] LHCb Collaboration, Prompt Λ_c^+ production in pPb collisions at $\sqrt{s_{NN}} = 5.02$ TeV, Tech. Rep. LHCb-CONF-2017-005. CERN-LHCb-CONF-2017-005, CERN, Geneva, Sep. 2017, <http://cds.cern.ch/record/2282379>.
- [23] ARGUS Collaboration, H. Albrecht, et al., Measurement of Ξ_c production in e^+e^- annihilation at 10.5-GeV center-of-mass energy, Phys. Lett. B 247 (1990) 121.
- [24] ARGUS Collaboration, H. Albrecht, et al., Observation of Ξ_c^0 semileptonic decay, Phys. Lett. B 303 (1993) 368.
- [25] CLEO Collaboration, J.P. Alexander, et al., First observation of $\Xi_c^+ \rightarrow \Xi_c^0 e^+ \nu_e$ and an estimate of the Ξ_c^+ / Ξ_c^0 lifetime ratio, Phys. Rev. Lett. 74 (1995) 3113; Phys. Rev. Lett. 75 (1995) 4155 (Erratum).
- [26] ARGUS Collaboration, H. Albrecht, et al., Evidence for W exchange in charmed baryon decays, Phys. Lett. B 342 (1995) 397.
- [27] BaBar Collaboration, B. Aubert, et al., Production and decay of Ξ_c^0 at BABAR, Phys. Rev. Lett. 95 (2005) 142003, arXiv:hep-ex/0504014.
- [28] J.R. Christiansen, P.Z. Skands, String formation beyond leading colour, J. High Energy Phys. 08 (2015) 003, arXiv:1505.01681 [hep-ph].
- [29] P.R. Sorensen, X. Dong, Suppression of non-photonic electrons from enhancement of charm baryons in heavy ion collisions, Phys. Rev. C 74 (2006) 024902, arXiv:nucl-th/0512042.
- [30] S.H. Lee, K. Ohnishi, S. Yasui, I.-K. Yoo, C.-M. Ko, Λ_c enhancement from strongly coupled quark–gluon plasma, Phys. Rev. Lett. 100 (2008) 222301, arXiv:0709.3637 [nucl-th].
- [31] G. Martinez-Garcia, S. Gadrat, P. Crochet, Consequences of a Λ_c/D enhancement effect on the non-photonic electron nuclear modification factor in central heavy ion collisions at RHIC energy, Phys. Lett. B 663 (2008) 55, arXiv:0710.2152 [hep-ph]; Phys. Lett. B 666 (2008) 533 (Erratum).
- [32] Y. Oh, C.M. Ko, S.H. Lee, S. Yasui, Heavy baryon/meson ratios in relativistic heavy ion collisions, Phys. Rev. C 79 (2009) 044905, arXiv:0901.1382 [nucl-th].
- [33] S. Ghosh, S.K. Das, V. Greco, S. Sarkar, J.-e. Alam, Diffusion of Λ_c in hot hadronic medium and its impact on Λ_c/D ratio, Phys. Rev. D 90 (2014) 054018, arXiv:1407.5069 [nucl-th].
- [34] Particle Data Group Collaboration, K.A. Olive, et al., Review of particle physics, Chin. Phys. C 40 (2016) 100001.
- [35] ALICE Collaboration, K. Aamodt, et al., The ALICE experiment at the CERN LHC, J. Instrum. 3 (2008) S08002.
- [36] ALICE Collaboration, B. Abelev, et al., Performance of the ALICE experiment at the CERN LHC, Int. J. Mod. Phys. A 29 (2014) 1430044, arXiv:1402.4476 [nucl-ex].
- [37] ALICE Collaboration, K. Aamodt, et al., Alignment of the ALICE Inner Tracking System with cosmic-ray tracks, J. Instrum. 5 (2010) P03003, arXiv:1001.0502 [physics.ins-det].
- [38] ALICE Collaboration, B. Abelev, et al., Measurement of charm production at central rapidity in proton–proton collisions at $\sqrt{s} = 7$ TeV, J. High Energy Phys. 01 (2012) 128, arXiv:1111.1553 [hep-ex].
- [39] J. Alme, et al., The ALICE TPC, a large 3-dimensional tracking device with fast readout for ultra-high multiplicity events, Nucl. Instrum. Methods Phys. Res., Sect. A 622 (2010) 316, arXiv:1001.1950 [physics.ins-det].
- [40] ALICE Collaboration, J. Adam, et al., Determination of the event collision time with the ALICE detector at the LHC, Eur. Phys. J. Plus 132 (2017) 99, arXiv:1610.03055 [physics.ins-det].
- [41] ALICE Collaboration, B. Abelev, et al., Measurement of inelastic, single- and double-diffraction cross sections in proton–proton collisions at the LHC with ALICE, Eur. Phys. J. C 73 (2013) 2456, arXiv:1208.4968 [hep-ex].
- [42] ALICE Collaboration, J. Adam, et al., Measurement of electrons from heavy-flavour hadron decays in p–Pb collisions at $\sqrt{s_{NN}} = 5.02$ TeV, Phys. Lett. B 754 (2016) 81, arXiv:1509.07491 [nucl-ex].
- [43] ALICE Collaboration, K. Aamodt, et al., Strange particle production in proton–proton collisions at $\sqrt{s} = 0.9$ TeV with ALICE at the LHC, Eur. Phys. J. C 71 (2011) 1594, arXiv:1012.3257 [hep-ex].
- [44] ALICE Collaboration, B. Abelev, et al., Multi-strange baryon production in pp collisions at $\sqrt{s} = 7$ TeV with ALICE, Phys. Lett. B 712 (2012) 309, arXiv:1204.0282 [nucl-ex].
- [45] ALICE Collaboration, B. Abelev, et al., Production of $\Sigma(1385)^\pm$ and $\Xi(1530)^0$ in proton–proton collisions at $\sqrt{s} = 7$ TeV, Eur. Phys. J. C 75 (2015) 1, arXiv:1406.3206 [nucl-ex].
- [46] T. Sjostrand, S. Mrenna, P.Z. Skands, PYTHIA 6.4 physics and manual, J. High Energy Phys. 05 (2006) 026, arXiv:hep-ph/0603175.
- [47] P.Z. Skands, The Perugia tunes, in: Proceedings, 1st International Workshop on Multiple Partonic Interactions at the LHC (MPI08), Perugia, Italy, October 27–31, 2008, 2009, p. 284, arXiv:0905.3418 [hep-ph].
- [48] R. Brun, F. Bruyant, F. Carminati, S. Giani, M. Maire, A. McPherson, G. Patrick, L. Urban, GEANT detector description and simulation tool, CERN-W5013, CERN-W-5013, W5013, W-5013.
- [49] CMS Collaboration, S. Chatrchyan, et al., Measurement of the Λ_b cross section and the $\bar{\Lambda}_b$ to Λ_b ratio with $J/\psi\Lambda$ decays in pp collisions at $\sqrt{s} = 7$ TeV, Phys. Lett. B 714 (2012) 136, arXiv:1205.0594 [hep-ex].
- [50] LHCb Collaboration, R. Aaij, et al., Study of the production of Λ_b^0 and \bar{B}^0 hadrons in pp collisions and first measurement of the $\Lambda_b^0 \rightarrow J/\psi p K^-$ branching fraction, Chin. Phys. C 40 (2016) 011001, arXiv:1509.00292 [hep-ex].
- [51] ALEPH Collaboration, D. Buskulic, et al., Strange b baryon production and lifetime in Z decays, Phys. Lett. B 384 (1996) 449.
- [52] ALEPH Collaboration, R. Barate, et al., Measurement of the B baryon lifetime and branching fractions in Z decays, Eur. Phys. J. C 2 (1998) 197.
- [53] CDF Collaboration, T. Aaltonen, et al., Measurement of ratios of fragmentation fractions for bottom hadrons in $p\bar{p}$ collisions at $\sqrt{s} = 1.96$ -TeV, Phys. Rev. D 77 (2008) 072003, arXiv:0801.4375 [hep-ex].
- [54] T. Adye, Unfolding algorithms and tests using RooUnfold, in: Proceedings, PHYSTAT 2011 Workshop on Statistical Issues Related to Discovery Claims in Search Experiments and Unfolding, CERN, Geneva, Switzerland 17–20 January 2011, CERN, Geneva, 2011, p. 313, arXiv:1105.1160 [physics.data-an].
- [55] G. D’Agostini, A multidimensional unfolding method based on Bayes’ theorem, Nucl. Instrum. Methods Phys. Res., Sect. A 362 (1995) 487.
- [56] ALICE Collaboration, E. Abbas, et al., Mid-rapidity anti-baryon to baryon ratios in pp collisions at $\sqrt{s} = 0.9, 2.76$ and 7 TeV measured by ALICE, Eur. Phys. J. C 73 (2013) 2496, arXiv:1305.1562 [nucl-ex].
- [57] GEANT4 Collaboration, S. Agostinelli, et al., GEANT4: a simulation toolkit, Nucl. Instrum. Methods Phys. Res., Sect. A 506 (2003) 250.
- [58] ALICE Collaboration, J.F. Grosse-Oetringhaus, Comments on unfolding methods in ALICE, in: Proceedings, PHYSTAT 2011 Workshop on Statistical Issues Related to Discovery Claims in Search Experiments and Unfolding, CERN, Geneva, Switzerland 17–20 January 2011, CERN, Geneva, 2011, p. 309, https://inspirehep.net/record/1478299/files/1087459_309-312.pdf.
- [59] V. Blobel, in: 8th CERN School of Comp. – CSC’84, Aiguablava, Spain, 9–22 Sep. 1984, CERN-85-09, 88, 1985.
- [60] A. Hocker, V. Kartvelishvili, SVD approach to data unfolding, Nucl. Instrum. Methods Phys. Res., Sect. A 372 (1996) 469, arXiv:hep-ph/9509307.
- [61] LHCb Collaboration, R. Aaij, et al., Precision measurement of the mass and lifetime of the Ξ_b^- baryon, Phys. Rev. Lett. 113 (2014) 242002, arXiv:1409.8568 [hep-ex].
- [62] P. Skands, S. Carrazza, J. Rojo, Tuning PYTHIA 8.1: the Monash 2013 tune, Eur. Phys. J. C 74 (2014) 3024, arXiv:1404.5630 [hep-ph].
- [63] C. Bierlich, J.R. Christiansen, Effects of color reconnection on hadron flavor observables, Phys. Rev. D 92 (9) (2015) 094010, arXiv:1507.02091 [hep-ph].
- [64] M. Bahr, et al., Herwig++ physics and manual, Eur. Phys. J. C 58 (2008) 639–707, arXiv:0803.0883 [hep-ph].
- [65] T. Sjostrand, S. Mrenna, P.Z. Skands, A brief introduction to PYTHIA 8.1, Comput. Phys. Commun. 178 (2008) 852, arXiv:0710.3820 [hep-ph].
- [66] B. Andersson, G. Gustafson, G. Ingelman, T. Sjostrand, Parton fragmentation and string dynamics, Phys. Rep. 97 (1983) 31.
- [67] T.S. Biro, H.B. Nielsen, J. Knoll, Color rope model for extreme relativistic heavy ion collisions, Nucl. Phys. B 245 (1984) 449–468.
- [68] B.R. Webber, A QCD model for jet fragmentation including soft gluon interference, Nucl. Phys. B 238 (1984) 492–528.
- [69] R. Perez-Marcial, R. Huerta, A. Garcia, M. Avila-Aoki, Predictions for semileptonic decays of charm baryons. 2. Nonrelativistic and MIT bag quark models, Phys. Rev. D 40 (1989) 2955; Phys. Rev. D 44 (1991) 2203 (Erratum).
- [70] R.L. Singleton, Semileptonic baryon decays with a heavy quark, Phys. Rev. D 43 (1991) 2939.
- [71] H.-Y. Cheng, B. Tseng, 1/M corrections to baryonic form-factors in the quark model, Phys. Rev. D 53 (1996) 1457, arXiv:hep-ph/9502391; Phys. Rev. D 55 (1997) 1697 (Erratum).

ALICE Collaboration

S. Acharya¹³⁷, D. Adamová⁹⁴, J. Adolfsson³⁴, M.M. Aggarwal⁹⁹, G. Aglieri Rinella³⁵, M. Agnello³¹, N. Agrawal⁴⁸, Z. Ahammed¹³⁷, S.U. Ahn⁷⁹, S. Aiola¹⁴¹, A. Akindinov⁶⁴, M. Al-Turany¹⁰⁶, S.N. Alam¹³⁷, D.S.D. Albuquerque¹²², D. Aleksandrov⁹⁰, B. Alessandro⁵⁸, R. Alfaro Molina⁷⁴, Y. Ali¹⁵, A. Alici^{12,53,27}, A. Alkin³, J. Alme²², T. Alt⁷⁰, L. Altenkamper²², I. Altsybeev¹³⁶, C. Alves Garcia Prado¹²¹, C. Andrei⁸⁷, D. Andreou³⁵, H.A. Andrews¹¹⁰, A. Andronic¹⁰⁶, V. Anguelov¹⁰⁴, C. Anson⁹⁷, T. Antičić¹⁰⁷, F. Antinori⁵⁶, P. Antonioli⁵³, L. Aphecetche¹¹⁴, H. Appelshäuser⁷⁰, S. Arcelli²⁷, R. Arnaldi⁵⁸, O.W. Arnold^{105,36}, I.C. Arsene²¹, M. Arslanodok¹⁰⁴, B. Audurier¹¹⁴, A. Augustinus³⁵, R. Averbeck¹⁰⁶, M.D. Azmi¹⁷, A. Badalà⁵⁵, Y.W. Baek^{60,78}, S. Bagnasco⁵⁸, R. Bailhache⁷⁰, R. Bala¹⁰¹, A. Baldisseri⁷⁵, M. Ball⁴⁵, R.C. Baral^{67,88}, A.M. Barbano²⁶, R. Barbera²⁸, F. Barile³³, L. Barioglio²⁶, G.G. Barnaföldi¹⁴⁰, L.S. Barnby⁹³, V. Barret¹³¹, P. Bartalini⁷, K. Barth³⁵, E. Bartsch⁷⁰, N. Bastid¹³¹, S. Basu¹³⁹, G. Batigne¹¹⁴, B. Batyunya⁷⁷, P.C. Batzing²¹, J.L. Bazo Alba¹¹¹, I.G. Bearden⁹¹, H. Beck¹⁰⁴, C. Bedda⁶³, N.K. Behera⁶⁰, I. Belikov¹³³, F. Bellini^{35,27}, H. Bello Martinez², R. Bellwied¹²⁴, L.G.E. Beltran¹²⁰, V. Belyaev⁸³, G. Bencedi¹⁴⁰, S. Beole²⁶, A. Bercuci⁸⁷, Y. Berdnikov⁹⁶, D. Berenyi¹⁴⁰, R.A. Bertens¹²⁷, D. Berzano^{58,35}, L. Betev³⁵, P.P. Bhaduri¹³⁷, A. Bhasin¹⁰¹, I.R. Bhat¹⁰¹, B. Bhattacharjee⁴⁴, J. Bhom¹¹⁸, A. Bianchi²⁶, L. Bianchi¹²⁴, N. Bianchi⁵¹, C. Bianchin¹³⁹, J. Bielčik³⁹, J. Bielčíková⁹⁴, A. Bilandzic^{36,105}, G. Biro¹⁴⁰, R. Biswas⁴, S. Biswas⁴, J.T. Blair¹¹⁹, D. Blau⁹⁰, C. Blume⁷⁰, G. Boca¹³⁴, F. Bock³⁵, A. Bogdanov⁸³, L. Boldizsár¹⁴⁰, M. Bombara⁴⁰, G. Bonomi¹³⁵, M. Bonora³⁵, H. Borel⁷⁵, A. Borissov^{104,19}, M. Borri¹²⁶, E. Botta²⁶, C. Bourjau⁹¹, L. Bratrud⁷⁰, P. Braun-Munzinger¹⁰⁶, M. Bregant¹²¹, T.A. Broker⁷⁰, M. Broz³⁹, E.J. Brucken⁴⁶, E. Bruna⁵⁸, G.E. Bruno^{35,33}, D. Budnikov¹⁰⁸, H. Buesching⁷⁰, S. Bufalino³¹, P. Buhler¹¹³, P. Buncic³⁵, O. Busch¹³⁰, Z. Buthelezi⁷⁶, J.B. Butt¹⁵, J.T. Buxton¹⁸, J. Cabala¹¹⁶, D. Caffarri^{35,92}, H. Caines¹⁴¹, A. Caliva^{106,63}, E. Calvo Villar¹¹¹, P. Camerini²⁵, A.A. Capon¹¹³, F. Carena³⁵, W. Carena³⁵, F. Carnesecchi^{12,27}, J. Castillo Castellanos⁷⁵, A.J. Castro¹²⁷, E.A.R. Casula⁵⁴, C. Ceballos Sanchez⁹, S. Chandra¹³⁷, B. Chang¹²⁵, W. Chang⁷, S. Chapeland³⁵, M. Chartier¹²⁶, S. Chattopadhyay¹³⁷, S. Chattopadhyay¹⁰⁹, A. Chauvin^{36,105}, C. Cheshkov¹³², B. Cheynis¹³², V. Chibante Barroso³⁵, D.D. Chinellato¹²², S. Cho⁶⁰, P. Chochula³⁵, M. Chojnacki⁹¹, S. Choudhury¹³⁷, T. Chowdhury¹³¹, P. Christakoglou⁹², C.H. Christensen⁹¹, P. Christiansen³⁴, T. Chujo¹³⁰, S.U. Chung¹⁹, C. Cicalo⁵⁴, L. Cifarelli^{12,27}, F. Cindolo⁵³, J. Cleymans¹⁰⁰, F. Colamaria^{52,33}, D. Colella^{52,35,65}, A. Collu⁸², M. Colocci²⁷, M. Concas^{58,ii}, G. Conesa Balbastre⁸¹, Z. Conesa del Valle⁶¹, J.G. Contreras³⁹, T.M. Cormier⁹⁵, Y. Corrales Morales⁵⁸, I. Cortés Maldonado², P. Cortese³², M.R. Cosentino¹²³, F. Costa³⁵, S. Costanza¹³⁴, J. Crkovská⁶¹, P. Crochet¹³¹, E. Cuautle⁷², L. Cunqueiro^{95,71}, T. Dahms^{36,105}, A. Dainese⁵⁶, M.C. Danisch¹⁰⁴, A. Danu⁶⁸, D. Das¹⁰⁹, I. Das¹⁰⁹, S. Das⁴, A. Dash⁸⁸, S. Dash⁴⁸, S. De⁴⁹, A. De Caro³⁰, G. de Cataldo⁵², C. de Conti¹²¹, J. de Cuveland⁴², A. De Falco²⁴, D. De Gruttola^{30,12}, N. De Marco⁵⁸, S. De Pasquale³⁰, R.D. De Souza¹²², H.F. Degenhardt¹²¹, A. Deisting^{106,104}, A. Deloff⁸⁶, C. Deplano⁹², P. Dhankher⁴⁸, D. Di Bari³³, A. Di Mauro³⁵, P. Di Nezza⁵¹, B. Di Ruzza⁵⁶, M.A. Diaz Corchero¹⁰, T. Dietel¹⁰⁰, P. Dillenseger⁷⁰, Y. Ding⁷, R. Divià³⁵, Ø. Djuvsland²², A. Dobrin³⁵, D. Domenicis Gimenez¹²¹, B. Dönigus⁷⁰, O. Dordic²¹, L.V.R. Doremalen⁶³, A.K. Dubey¹³⁷, A. Dubla¹⁰⁶, L. Ducroux¹³², S. Dudi⁹⁹, A.K. Duggal⁹⁹, M. Dukhishyam⁸⁸, P. Dupieux¹³¹, R.J. Ehlers¹⁴¹, D. Elia⁵², E. Endress¹¹¹, H. Engel⁶⁹, E. Epple¹⁴¹, B. Erazmus¹¹⁴, F. Erhardt⁹⁸, B. Espagnon⁶¹, G. Eulisse³⁵, J. Eum¹⁹, D. Evans¹¹⁰, S. Evdokimov¹¹², L. Fabbietti^{105,36}, J. Faivre⁸¹, A. Fantoni⁵¹, M. Fasel⁹⁵, L. Feldkamp⁷¹, A. Feliciello⁵⁸, G. Feofilov¹³⁶, A. Fernández Téllez², E.G. Ferreira¹⁶, A. Ferretti²⁶, A. Festanti^{29,35}, V.J.G. Feuillard^{75,131}, J. Figiel¹¹⁸, M.A.S. Figueredo¹²¹, S. Filchagin¹⁰⁸, D. Finogeev⁶², F.M. Fionda^{22,24}, M. Floris³⁵, S. Foertsch⁷⁶, P. Foka¹⁰⁶, S. Fokin⁹⁰, E. Fragiaco⁵⁹, A. Francescon³⁵, A. Francisco¹¹⁴, U. Frankenfeld¹⁰⁶, G.G. Fronze²⁶, U. Fuchs³⁵, C. Furget⁸¹, A. Furs⁶², M. Fusco Girard³⁰, J.J. Gaardhøje⁹¹, M. Gagliardi²⁶, A.M. Gago¹¹¹, K. Gajdosova⁹¹, M. Gallio²⁶, C.D. Galvan¹²⁰, P. Ganoti⁸⁵, C. Garabatos¹⁰⁶, E. Garcia-Solis¹³, K. Garg²⁸, C. Gargiulo³⁵, P. Gasik^{105,36}, E.F. Gauger¹¹⁹, M.B. Gay Ducati⁷³, M. Germain¹¹⁴, J. Ghosh¹⁰⁹, P. Ghosh¹³⁷, S.K. Ghosh⁴, P. Gianotti⁵¹, P. Giubellino^{35,106,58}, P. Giubilato²⁹, E. Gladysz-Dziadus¹¹⁸, P. Glässel¹⁰⁴, D.M. Gómez Coral⁷⁴, A. Gomez Ramirez⁶⁹, A.S. Gonzalez³⁵, V. Gonzalez¹⁰, P. González-Zamora^{10,2}, S. Gorbunov⁴², L. Görlich¹¹⁸, S. Gotovac¹¹⁷, V. Grabski⁷⁴, L.K. Graczykowski¹³⁸, K.L. Graham¹¹⁰, L. Greiner⁸², A. Grelli⁶³, C. Grigoras³⁵, V. Grigoriev⁸³, A. Grigoryan¹, S. Grigoryan⁷⁷, J.M. Gronefeld¹⁰⁶, F. Grosa³¹, J.F. Grosse-Oetringhaus³⁵, R. Grosso¹⁰⁶, F. Guber⁶², R. Guernane⁸¹, B. Guerzoni²⁷, M. Guittiere¹¹⁴,

K. Gulbrandsen⁹¹, T. Gunji¹²⁹, A. Gupta¹⁰¹, R. Gupta¹⁰¹, I.B. Guzman², R. Haake³⁵, C. Hadjidakis⁶¹,
 H. Hamagaki⁸⁴, G. Hamar¹⁴⁰, J.C. Hamon¹³³, M.R. Haque⁶³, J.W. Harris¹⁴¹, A. Harton¹³, H. Hassan⁸¹,
 D. Hatzifotiadou^{53,12}, S. Hayashi¹²⁹, S.T. Heckel⁷⁰, E. Hellbär⁷⁰, H. Helstrup³⁷, A. Herghelegiu⁸⁷,
 E.G. Hernandez², G. Herrera Corral¹¹, F. Herrmann⁷¹, B.A. Hess¹⁰³, K.F. Hetland³⁷, H. Hillemanns³⁵,
 C. Hills¹²⁶, B. Hippolyte¹³³, B. Hohlweger¹⁰⁵, D. Horak³⁹, S. Hornung¹⁰⁶, R. Hosokawa^{130,81},
 P. Hristov³⁵, C. Hughes¹²⁷, T.J. Humanic¹⁸, N. Hussain⁴⁴, T. Hussain¹⁷, D. Hutter⁴², D.S. Hwang²⁰,
 J.P. Iddon¹²⁶, S.A. Iga Buitron⁷², R. Ilkaev¹⁰⁸, M. Inaba¹³⁰, M. Ippolitov^{83,90}, M.S. Islam¹⁰⁹,
 M. Ivanov¹⁰⁶, V. Ivanov⁹⁶, V. Izucheev¹¹², B. Jacak⁸², N. Jacazio²⁷, P.M. Jacobs⁸², M.B. Jadhav⁴⁸,
 S. Jadlovská¹¹⁶, J. Jadlovsky¹¹⁶, S. Jaelani⁶³, C. Jahnke³⁶, M.J. Jakubowska¹³⁸, M.A. Janik¹³⁸,
 P.H.S.Y. Jayarathna¹²⁴, C. Jena⁸⁸, M. Jercic⁹⁸, R.T. Jimenez Bustamante¹⁰⁶, P.G. Jones¹¹⁰, A. Jusko¹¹⁰,
 P. Kalinak⁶⁵, A. Kalweit³⁵, J.H. Kang¹⁴², V. Kaplin⁸³, S. Kar¹³⁷, A. Karasu Uysal⁸⁰, O. Karavichev⁶²,
 T. Karavicheva⁶², L. Karayan^{106,104}, P. Karczmarczyk³⁵, E. Karpechev⁶², U. Kebschull⁶⁹, R. Keidel¹⁴³,
 D.L.D. Keijdener⁶³, M. Keil³⁵, B. Ketzer⁴⁵, Z. Khabanova⁹², P. Khan¹⁰⁹, S. Khan¹⁷, S.A. Khan¹³⁷,
 A. Khanzadeev⁹⁶, Y. Kharlov¹¹², A. Khatun¹⁷, A. Khuntia⁴⁹, M.M. Kielbowicz¹¹⁸, B. Kileng³⁷, B. Kim¹³⁰,
 D. Kim¹⁴², D.J. Kim¹²⁵, H. Kim¹⁴², J.S. Kim⁴³, J. Kim¹⁰⁴, M. Kim⁶⁰, S. Kim²⁰, T. Kim¹⁴², S. Kirsch⁴²,
 I. Kisel⁴², S. Kiselev⁶⁴, A. Kisiel¹³⁸, G. Kiss¹⁴⁰, J.L. Klay⁶, C. Klein⁷⁰, J. Klein³⁵, C. Klein-Bösing⁷¹,
 S. Klewin¹⁰⁴, A. Kluge³⁵, M.L. Knichel^{104,35}, A.G. Knospe¹²⁴, C. Kobdaj¹¹⁵, M. Kofarago¹⁴⁰,
 M.K. Köhler¹⁰⁴, T. Kollegger¹⁰⁶, V. Kondratiev¹³⁶, N. Kondratyeva⁸³, E. Kondratyuk¹¹², A. Konevskikh⁶²,
 M. Konyushikhin¹³⁹, M. Kopicik¹¹⁶, M. Kour¹⁰¹, C. Kouzinopoulos³⁵, O. Kovalenko⁸⁶, V. Kovalenko¹³⁶,
 M. Kowalski¹¹⁸, G. Koyithatta Meethaleveedu⁴⁸, I. Králik⁶⁵, A. Kravčáková⁴⁰, L. Kreis¹⁰⁶,
 M. Krivda^{110,65}, F. Krizek⁹⁴, E. Kryshen⁹⁶, M. Krzewicki⁴², A.M. Kubera¹⁸, V. Kučera⁹⁴, C. Kuhn¹³³,
 P.G. Kuijer⁹², A. Kumar¹⁰¹, J. Kumar⁴⁸, L. Kumar⁹⁹, S. Kumar⁴⁸, S. Kundu⁸⁸, P. Kurashvili⁸⁶,
 A. Kurepin⁶², A.B. Kurepin⁶², A. Kuryakin¹⁰⁸, S. Kushpil⁹⁴, M.J. Kweon⁶⁰, Y. Kwon¹⁴², S.L. La Pointe⁴²,
 P. La Rocca²⁸, C. Lagana Fernandes¹²¹, Y.S. Lai⁸², I. Lakomov³⁵, R. Langoy⁴¹, K. Lapidus¹⁴¹, C. Lara⁶⁹,
 A. Lardeux²¹, A. Lattuca²⁶, E. Laudi³⁵, R. Lavicka³⁹, R. Lea²⁵, L. Leardini¹⁰⁴, S. Lee¹⁴², F. Lehas⁹²,
 S. Lehner¹¹³, J. Lehrbach⁴², R.C. Lemmon⁹³, E. Leogrande⁶³, I. León Monzón¹²⁰, P. Lévai¹⁴⁰, X. Li¹⁴,
 X.L. Li⁷, J. Lien⁴¹, R. Lietava¹¹⁰, B. Lim¹⁹, S. Lindal²¹, V. Lindenstruth⁴², S.W. Lindsay¹²⁶,
 C. Lippmann¹⁰⁶, M.A. Lisa¹⁸, V. Litichevskiy⁴⁶, A. Liu⁸², W.J. Llope¹³⁹, D.F. Lodato⁶³, P.I. Loenne²²,
 V. Loginov⁸³, C. Loizides^{82,95}, P. Loncar¹¹⁷, X. Lopez¹³¹, E. López Torres⁹, A. Lowe¹⁴⁰, P. Luettig⁷⁰,
 J.R. Luhder⁷¹, M. Lunardon²⁹, G. Luparello^{25,59}, M. Lupi³⁵, T.H. Lutz¹⁴¹, A. Maevskaya⁶², M. Mager³⁵,
 S.M. Mahmood²¹, A. Maire¹³³, R.D. Majka¹⁴¹, M. Malaev⁹⁶, L. Malinina^{77,iii}, D. Mal'Kevich⁶⁴,
 P. Malzacher¹⁰⁶, A. Mamonov¹⁰⁸, V. Manko⁹⁰, F. Manso¹³¹, V. Manzari⁵², Y. Mao⁷,
 M. Marchisone^{128,132,76}, J. Mareš⁶⁶, G.V. Margagliotti²⁵, A. Margotti⁵³, J. Margutti⁶³, A. Marín¹⁰⁶,
 C. Markert¹¹⁹, M. Marquard⁷⁰, N.A. Martin¹⁰⁶, P. Martinengo³⁵, J.A.L. Martinez⁶⁹, M.I. Martínez²,
 G. Martínez García¹¹⁴, M. Martinez Pedreira³⁵, S. Masciocchi¹⁰⁶, M. Maserà²⁶, A. Masoni⁵⁴,
 L. Massacrier⁶¹, E. Masson¹¹⁴, A. Mastroserio⁵², A.M. Mathis^{36,105}, P.F.T. Matuoka¹²¹, A. Matyja¹²⁷,
 C. Mayer¹¹⁸, J. Mazer¹²⁷, M. Mazzilli³³, M.A. Mazzoni⁵⁷, F. Meddi²³, Y. Melikyan⁸³,
 A. Menchaca-Rocha⁷⁴, E. Meninno³⁰, J. Mercado Pérez¹⁰⁴, M. Meres³⁸, S. Mhlanga¹⁰⁰, Y. Miale¹³⁰,
 M.M. Mieskolainen⁴⁶, D.L. Mihaylov¹⁰⁵, K. Mikhaylov^{77,64}, A. Mischke⁶³, A.N. Mishra⁴⁹,
 D. Miśkowiec¹⁰⁶, J. Mitra¹³⁷, C.M. Mitu⁶⁸, N. Mohammadi^{63,35}, A.P. Mohanty⁶³, B. Mohanty⁸⁸,
 M. Mohisin Khan^{17,iv}, E. Montes¹⁰, D.A. Moreira De Godoy⁷¹, L.A.P. Moreno², S. Moretto²⁹,
 A. Morreale¹¹⁴, A. Morsch³⁵, V. Muccifora⁵¹, E. Mudnic¹¹⁷, D. Mühlheim⁷¹, S. Muhuri¹³⁷,
 J.D. Mulligan¹⁴¹, M.G. Munhoz¹²¹, K. Munning⁴⁵, R.H. Munzer⁷⁰, H. Murakami¹²⁹, S. Murray⁷⁶,
 L. Musa³⁵, J. Musinsky⁶⁵, C.J. Myers¹²⁴, J.W. Myrcha¹³⁸, D. Nag⁴, B. Naik⁴⁸, R. Nair⁸⁶, B.K. Nandi⁴⁸,
 R. Nania^{12,53}, E. Nappi⁵², A. Narayan⁴⁸, M.U. Naru¹⁵, H. Natal da Luz¹²¹, C. Nattrass¹²⁷, S.R. Navarro²,
 K. Nayak⁸⁸, R. Nayak⁴⁸, T.K. Nayak¹³⁷, S. Nazarenko¹⁰⁸, R.A. Negrao De Oliveira^{70,35}, L. Nellen⁷²,
 S.V. Nesbo³⁷, G. Neskovic⁴², F. Ng¹²⁴, M. Nicassio¹⁰⁶, M. Niculescu⁶⁸, J. Niedziela^{138,35}, B.S. Nielsen⁹¹,
 S. Nikolaev⁹⁰, S. Nikulin⁹⁰, V. Nikulin⁹⁶, A. Nobuhiro⁴⁷, F. Noferini^{12,53}, P. Nomokonov⁷⁷, G. Nooren⁶³,
 J.C.C. Noris², J. Norman^{81,126}, A. Nyanin⁹⁰, J. Nystrand²², H. Oeschler^{19,104,i}, H. Oh¹⁴², A. Ohlson¹⁰⁴,
 L. Olah¹⁴⁰, J. Oleniacz¹³⁸, A.C. Oliveira Da Silva¹²¹, M.H. Oliver¹⁴¹, J. Onderwaater¹⁰⁶, C. Oppedisano⁵⁸,
 R. Orava⁴⁶, M. Oravec¹¹⁶, A. Ortiz Velasquez⁷², A. Oskarsson³⁴, J. Otwinowski¹¹⁸, K. Oyama⁸⁴,
 Y. Pachmayer¹⁰⁴, V. Pacik⁹¹, D. Pagano¹³⁵, G. Paic⁷², P. Palni⁷, J. Pan¹³⁹, A.K. Pandey⁴⁸,

S. Panebianco⁷⁵, V. Papikyan¹, P. Pareek⁴⁹, J. Park⁶⁰, S. Parmar⁹⁹, A. Passfeld⁷¹, S.P. Pathak¹²⁴,
 R.N. Patra¹³⁷, B. Paul⁵⁸, H. Pei⁷, T. Peitzmann⁶³, X. Peng⁷, L.G. Pereira⁷³, H. Pereira Da Costa⁷⁵,
 D. Peresunko^{83,90}, E. Perez Lezama⁷⁰, V. Peskov⁷⁰, Y. Pestov⁵, V. Petráček³⁹, M. Petrovici⁸⁷, C. Petta²⁸,
 R.P. Pezzi⁷³, S. Piano⁵⁹, M. Pikna³⁸, P. Pillot¹¹⁴, L.O.D.L. Pimentel⁹¹, O. Pinazza^{53,35}, L. Pinsky¹²⁴,
 D.B. Piyarathna¹²⁴, M. Płoskoń⁸², M. Planinic⁹⁸, F. Pliquett⁷⁰, J. Pluta¹³⁸, S. Pochybova¹⁴⁰,
 P.L.M. Podesta-Lerma¹²⁰, M.G. Poghosyan⁹⁵, B. Polichtchouk¹¹², N. Poljak⁹⁸, W. Poonsawat¹¹⁵, A. Pop⁸⁷,
 H. Poppenborg⁷¹, S. Porteboeuf-Houssais¹³¹, V. Pozdniakov⁷⁷, S.K. Prasad⁴, R. Preghenella⁵³, F. Prino⁵⁸,
 C.A. Pruneau¹³⁹, I. Pshenichnov⁶², M. Puccio²⁶, V. Punin¹⁰⁸, J. Putschke¹³⁹, S. Raha⁴, S. Rajput¹⁰¹,
 J. Rak¹²⁵, A. Rakotozafindrabe⁷⁵, L. Ramello³², F. Rami¹³³, D.B. Rana¹²⁴, R. Raniwala¹⁰², S. Raniwala¹⁰²,
 S.S. Räsänen⁴⁶, B.T. Rascanu⁷⁰, D. Rathee⁹⁹, V. Ratzka⁴⁵, I. Ravasenga³¹, K.F. Read^{127,95}, K. Redlich^{86,v},
 A. Rehman²², P. Reichelt⁷⁰, F. Reidt³⁵, X. Ren⁷, R. Renfordt⁷⁰, A. Reshetin⁶², K. Reygers¹⁰⁴, V. Riabov⁹⁶,
 T. Richert^{63,34}, M. Richter²¹, P. Riedler³⁵, W. Riegler³⁵, F. Riggi²⁸, C. Ristea⁶⁸, M. Rodríguez Cahuantzi²,
 K. Røed²¹, R. Rogalev¹¹², E. Rogochaya⁷⁷, D. Rohr^{35,42}, D. Röhrich²², P.S. Rokita¹³⁸, F. Ronchetti⁵¹,
 E.D. Rosas⁷², K. Roslon¹³⁸, P. Rosnet¹³¹, A. Rossi^{56,29}, A. Rotondi¹³⁴, F. Roukoutakis⁸⁵, C. Roy¹³³,
 P. Roy¹⁰⁹, A.J. Rubio Montero¹⁰, O.V. Rueda⁷², R. Rui²⁵, B. Rumyantsev⁷⁷, A. Rustamov⁸⁹,
 E. Ryabinkin⁹⁰, Y. Ryabov⁹⁶, A. Rybicki¹¹⁸, S. Saarinen⁴⁶, S. Sadhu¹³⁷, S. Sadosky¹¹², K. Šafařík³⁵,
 S.K. Saha¹³⁷, B. Sahlmuller⁷⁰, B. Sahoo⁴⁸, P. Sahoo⁴⁹, R. Sahoo⁴⁹, S. Sahoo⁶⁷, P.K. Sahu⁶⁷, J. Saini¹³⁷,
 S. Sakai¹³⁰, M.A. Saleh¹³⁹, J. Salzwedel¹⁸, S. Sambyal¹⁰¹, V. Samsonov^{96,83}, A. Sandoval⁷⁴, A. Sarkar⁷⁶,
 D. Sarkar¹³⁷, N. Sarkar¹³⁷, P. Sarma⁴⁴, M.H.P. Sas⁶³, E. Scapparone⁵³, F. Scarlassara²⁹, B. Schaefer⁹⁵,
 H.S. Scheid⁷⁰, C. Schiaua⁸⁷, R. Schicker¹⁰⁴, C. Schmidt¹⁰⁶, H.R. Schmidt¹⁰³, M.O. Schmidt¹⁰⁴,
 M. Schmidt¹⁰³, N.V. Schmidt^{95,70}, J. Schukraft³⁵, Y. Schutz^{35,133}, K. Schwarz¹⁰⁶, K. Schweda¹⁰⁶,
 G. Scioli²⁷, E. Scomparin⁵⁸, M. Šefčík⁴⁰, J.E. Seger⁹⁷, Y. Sekiguchi¹²⁹, D. Sekihata⁴⁷,
 I. Selyuzhenkov^{106,83}, K. Senosi⁷⁶, S. Senyukov¹³³, E. Serradilla^{10,74}, P. Sett⁴⁸, A. Sevcenco⁶⁸,
 A. Shabanov⁶², A. Shabetai¹¹⁴, R. Shahoyan³⁵, W. Shaikh¹⁰⁹, A. Shangaraev¹¹², A. Sharma⁹⁹,
 A. Sharma¹⁰¹, M. Sharma¹⁰¹, M. Sharma¹⁰¹, N. Sharma⁹⁹, A.I. Sheikh¹³⁷, K. Shigaki⁴⁷, S. Shirinkin⁶⁴,
 Q. Shou⁷, K. Shtejer^{9,26}, Y. Sibiriak⁹⁰, S. Siddhanta⁵⁴, K.M. Sielewicz³⁵, T. Siemiarczuk⁸⁶, S. Silaeva⁹⁰,
 D. Silvermyr³⁴, G. Simatovic⁹², G. Simonetti³⁵, R. Singaraju¹³⁷, R. Singh⁸⁸, V. Singhal¹³⁷, T. Sinha¹⁰⁹,
 B. Sitar³⁸, M. Sitta³², T.B. Skaali²¹, M. Slupecki¹²⁵, N. Smirnov¹⁴¹, R.J.M. Snellings⁶³, T.W. Snellman¹²⁵,
 J. Song¹⁹, M. Song¹⁴², F. Soramel²⁹, S. Sorensen¹²⁷, F. Sozzi¹⁰⁶, I. Sputowska¹¹⁸, J. Stachel¹⁰⁴, I. Stan⁶⁸,
 P. Stankus⁹⁵, E. Stenlund³⁴, D. Stocco¹¹⁴, M.M. Storetvedt³⁷, P. Strmen³⁸, A.A.P. Suaide¹²¹, T. Sugitate⁴⁷,
 C. Suire⁶¹, M. Suleymanov¹⁵, M. Suljic²⁵, R. Sultanov⁶⁴, M. Šumbera⁹⁴, S. Sumowidagdo⁵⁰,
 K. Suzuki¹¹³, S. Swain⁶⁷, A. Szabo³⁸, I. Szarka³⁸, U. Tabassam¹⁵, J. Takahashi¹²², G.J. Tambave²²,
 N. Tanaka¹³⁰, M. Tarhini^{114,61}, M. Tariq¹⁷, M.G. Tarzila⁸⁷, A. Tauro³⁵, G. Tejada Muñoz², A. Telesca³⁵,
 K. Terasaki¹²⁹, C. Terrevoli²⁹, B. Teyssier¹³², D. Thakur⁴⁹, S. Thakur¹³⁷, D. Thomas¹¹⁹, F. Thoresen⁹¹,
 R. Tieulent¹³², A. Tikhonov⁶², A.R. Timmins¹²⁴, A. Toia⁷⁰, M. Toppi⁵¹, S.R. Torres¹²⁰, S. Tripathy⁴⁹,
 S. Trogolo²⁶, G. Trombetta³³, L. Tropp⁴⁰, V. Trubnikov³, W.H. Trzaska¹²⁵, B.A. Trzeciak⁶³, T. Tsuji¹²⁹,
 A. Tumkin¹⁰⁸, R. Turrisi⁵⁶, T.S. Tveter²¹, K. Ullaland²², E.N. Umaka¹²⁴, A. Uras¹³², G.L. Usai²⁴,
 A. Utrobicic⁹⁸, M. Vala^{116,65}, J. Van Der Maarel⁶³, J.W. Van Hoorne³⁵, M. van Leeuwen⁶³, T. Vanat⁹⁴,
 P. Vande Vyvre³⁵, D. Varga¹⁴⁰, A. Vargas², M. Vargyas¹²⁵, R. Varma⁴⁸, M. Vasileiou⁸⁵, A. Vasiliev⁹⁰,
 A. Vauthier⁸¹, O. Vázquez Doce^{105,36}, V. Vechernin¹³⁶, A.M. Veen⁶³, A. Velure²², E. Vercellin²⁶,
 S. Vergara Limón², L. Vermunt⁶³, R. Vernet⁸, R. Vértesi¹⁴⁰, L. Vickovic¹¹⁷, S. Vigolo⁶³, J. Viinikainen¹²⁵,
 Z. Vilakazi¹²⁸, O. Villalobos Baillie¹¹⁰, A. Villatoro Tello², A. Vinogradov⁹⁰, L. Vinogradov¹³⁶, T. Virgili³⁰,
 V. Vislavicius³⁴, A. Vodopyanov⁷⁷, M.A. Völkl¹⁰³, K. Voloshin⁶⁴, S.A. Voloshin¹³⁹, G. Volpe³³,
 B. von Haller³⁵, I. Vorobyev^{105,36}, D. Voscek¹¹⁶, D. Vranic^{35,106}, J. Vrláková⁴⁰, B. Wagner²², H. Wang⁶³,
 M. Wang⁷, Y. Watanabe^{129,130}, M. Weber¹¹³, S.G. Weber¹⁰⁶, A. Wegrzynek³⁵, D.F. Weiser¹⁰⁴,
 S.C. Wenzel³⁵, J.P. Wessels⁷¹, U. Westerhoff⁷¹, A.M. Whitehead¹⁰⁰, J. Wiechula⁷⁰, J. Wikne²¹, G. Wilk⁸⁶,
 J. Wilkinson^{104,53}, G.A. Willems^{71,35}, M.C.S. Williams⁵³, E. Willsher¹¹⁰, B. Windelband¹⁰⁴, W.E. Witt¹²⁷,
 R. Xu⁷, S. Yalcin⁸⁰, K. Yamakawa⁴⁷, P. Yang⁷, S. Yano⁴⁷, Z. Yin⁷, H. Yokoyama^{81,130}, I.-K. Yoo¹⁹,
 J.H. Yoon⁶⁰, E. Yun¹⁹, V. Yurchenko³, V. Zaccolo⁵⁸, A. Zaman¹⁵, C. Zampolli³⁵, H.J.C. Zanoli¹²¹,
 N. Zardoshti¹¹⁰, A. Zarochentsev¹³⁶, P. Závada⁶⁶, N. Zaviyalov¹⁰⁸, H. Zbroszczyk¹³⁸, M. Zhalov⁹⁶,
 H. Zhang^{7,22}, X. Zhang⁷, Y. Zhang⁷, C. Zhang⁶³, Z. Zhang^{131,7}, C. Zhao²¹, N. Zhigareva⁶⁴, D. Zhou⁷,

Y. Zhou⁹¹, Z. Zhou²², H. Zhu²², J. Zhu⁷, Y. Zhu⁷, A. Zichichi^{27,12}, M.B. Zimmermann³⁵, G. Zinovjev³, J. Zmeskal¹¹³, S. Zou⁷

¹ A.I. Alikhanyan National Science Laboratory (Yerevan Physics Institute) Foundation, Yerevan, Armenia

² Benemérita Universidad Autónoma de Puebla, Puebla, Mexico

³ Bogolyubov Institute for Theoretical Physics, Kiev, Ukraine

⁴ Bose Institute, Department of Physics and Centre for Astroparticle Physics and Space Science (CAPSS), Kolkata, India

⁵ Budker Institute for Nuclear Physics, Novosibirsk, Russia

⁶ California Polytechnic State University, San Luis Obispo, CA, United States

⁷ Central China Normal University, Wuhan, China

⁸ Centre de Calcul de l'IN2P3, Villeurbanne, Lyon, France

⁹ Centro de Aplicaciones Tecnológicas y Desarrollo Nuclear (CEADEN), Havana, Cuba

¹⁰ Centro de Investigaciones Energéticas Medioambientales y Tecnológicas (CIEMAT), Madrid, Spain

¹¹ Centro de Investigación y de Estudios Avanzados (CINVESTAV), Mexico City and Mérida, Mexico

¹² Centro Fermi – Museo Storico della Fisica e Centro Studi e Ricerche “Enrico Fermi”, Rome, Italy

¹³ Chicago State University, Chicago, IL, United States

¹⁴ China Institute of Atomic Energy, Beijing, China

¹⁵ COMSATS Institute of Information Technology (CIIT), Islamabad, Pakistan

¹⁶ Departamento de Física de Partículas and IGFAE, Universidad de Santiago de Compostela, Santiago de Compostela, Spain

¹⁷ Department of Physics, Aligarh Muslim University, Aligarh, India

¹⁸ Department of Physics, Ohio State University, Columbus, OH, United States

¹⁹ Department of Physics, Pusan National University, Pusan, Republic of Korea

²⁰ Department of Physics, Sejong University, Seoul, Republic of Korea

²¹ Department of Physics, University of Oslo, Oslo, Norway

²² Department of Physics and Technology, University of Bergen, Bergen, Norway

²³ Dipartimento di Fisica dell'Università ‘La Sapienza’ and Sezione INFN, Rome, Italy

²⁴ Dipartimento di Fisica dell'Università and Sezione INFN, Cagliari, Italy

²⁵ Dipartimento di Fisica dell'Università and Sezione INFN, Trieste, Italy

²⁶ Dipartimento di Fisica dell'Università and Sezione INFN, Turin, Italy

²⁷ Dipartimento di Fisica e Astronomia dell'Università and Sezione INFN, Bologna, Italy

²⁸ Dipartimento di Fisica e Astronomia dell'Università and Sezione INFN, Catania, Italy

²⁹ Dipartimento di Fisica e Astronomia dell'Università and Sezione INFN, Padova, Italy

³⁰ Dipartimento di Fisica ‘E.R. Caianiello’ dell'Università and Gruppo Collegato INFN, Salerno, Italy

³¹ Dipartimento DISAT del Politecnico and Sezione INFN, Turin, Italy

³² Dipartimento di Scienze e Innovazione Tecnologica dell'Università del Piemonte Orientale and INFN Sezione di Torino, Alessandria, Italy

³³ Dipartimento Interateneo di Fisica ‘M. Merlin’ and Sezione INFN, Bari, Italy

³⁴ Division of Experimental High Energy Physics, University of Lund, Lund, Sweden

³⁵ European Organization for Nuclear Research (CERN), Geneva, Switzerland

³⁶ Excellence Cluster Universe, Technische Universität München, Munich, Germany

³⁷ Faculty of Engineering, Bergen University College, Bergen, Norway

³⁸ Faculty of Mathematics, Physics and Informatics, Comenius University, Bratislava, Slovakia

³⁹ Faculty of Nuclear Sciences and Physical Engineering, Czech Technical University in Prague, Prague, Czech Republic

⁴⁰ Faculty of Science, P.J. Šafárik University, Košice, Slovakia

⁴¹ Faculty of Technology, Buskerud and Vestfold University College, Tonsberg, Norway

⁴² Frankfurt Institute for Advanced Studies, Johann Wolfgang Goethe-Universität Frankfurt, Frankfurt, Germany

⁴³ Gangneung-Wonju National University, Gangneung, Republic of Korea

⁴⁴ Gauhati University, Department of Physics, Guwahati, India

⁴⁵ Helmholtz-Institut für Strahlen- und Kernphysik, Rheinische Friedrich-Wilhelms-Universität Bonn, Bonn, Germany

⁴⁶ Helsinki Institute of Physics (HIP), Helsinki, Finland

⁴⁷ Hiroshima University, Hiroshima, Japan

⁴⁸ Indian Institute of Technology Bombay (IIT), Mumbai, India

⁴⁹ Indian Institute of Technology Indore, Indore, India

⁵⁰ Indonesian Institute of Sciences, Jakarta, Indonesia

⁵¹ INFN, Laboratori Nazionali di Frascati, Frascati, Italy

⁵² INFN, Sezione di Bari, Bari, Italy

⁵³ INFN, Sezione di Bologna, Bologna, Italy

⁵⁴ INFN, Sezione di Cagliari, Cagliari, Italy

⁵⁵ INFN, Sezione di Catania, Catania, Italy

⁵⁶ INFN, Sezione di Padova, Padova, Italy

⁵⁷ INFN, Sezione di Roma, Rome, Italy

⁵⁸ INFN, Sezione di Torino, Turin, Italy

⁵⁹ INFN, Sezione di Trieste, Trieste, Italy

⁶⁰ Inha University, Incheon, Republic of Korea

⁶¹ Institut de Physique Nucléaire d'Orsay (IPNO), Université Paris-Sud, CNRS-IN2P3, Orsay, France

⁶² Institute for Nuclear Research, Academy of Sciences, Moscow, Russia

⁶³ Institute for Subatomic Physics of Utrecht University, Utrecht, Netherlands

⁶⁴ Institute for Theoretical and Experimental Physics, Moscow, Russia

⁶⁵ Institute of Experimental Physics, Slovak Academy of Sciences, Košice, Slovakia

⁶⁶ Institute of Physics, Academy of Sciences of the Czech Republic, Prague, Czech Republic

⁶⁷ Institute of Physics, Bhubaneswar, India

⁶⁸ Institute of Space Science (ISS), Bucharest, Romania

⁶⁹ Institut für Informatik, Johann Wolfgang Goethe-Universität Frankfurt, Frankfurt, Germany

⁷⁰ Institut für Kernphysik, Johann Wolfgang Goethe-Universität Frankfurt, Frankfurt, Germany

⁷¹ Institut für Kernphysik, Westfälische Wilhelms-Universität Münster, Münster, Germany

⁷² Instituto de Ciencias Nucleares, Universidad Nacional Autónoma de México, Mexico City, Mexico

⁷³ Instituto de Física, Universidade Federal do Rio Grande do Sul (UFRGS), Porto Alegre, Brazil

⁷⁴ Instituto de Física, Universidad Nacional Autónoma de México, Mexico City, Mexico

⁷⁵ IRFU, CEA, Université Paris-Saclay, Saclay, France

- 76 iThemba LABS, National Research Foundation, Somerset West, South Africa
- 77 Joint Institute for Nuclear Research (JINR), Dubna, Russia
- 78 Konkuk University, Seoul, Republic of Korea
- 79 Korea Institute of Science and Technology Information, Daejeon, Republic of Korea
- 80 KTO Karatay University, Konya, Turkey
- 81 Laboratoire de Physique Subatomique et de Cosmologie, Université Grenoble-Alpes, CNRS-IN2P3, Grenoble, France
- 82 Lawrence Berkeley National Laboratory, Berkeley, CA, United States
- 83 Moscow Engineering Physics Institute, Moscow, Russia
- 84 Nagasaki Institute of Applied Science, Nagasaki, Japan
- 85 National and Kapodistrian University of Athens, Physics Department, Athens, Greece
- 86 National Centre for Nuclear Studies, Warsaw, Poland
- 87 National Institute for Physics and Nuclear Engineering, Bucharest, Romania
- 88 National Institute of Science Education and Research, HBNI, Jatni, India
- 89 National Nuclear Research Center, Baku, Azerbaijan
- 90 National Research Centre Kurchatov Institute, Moscow, Russia
- 91 Niels Bohr Institute, University of Copenhagen, Copenhagen, Denmark
- 92 Nikhef, Nationaal instituut voor subatomaire fysica, Amsterdam, Netherlands
- 93 Nuclear Physics Group, STFC Daresbury Laboratory, Daresbury, United Kingdom
- 94 Nuclear Physics Institute, Academy of Sciences of the Czech Republic, Řež u Prahy, Czech Republic
- 95 Oak Ridge National Laboratory, Oak Ridge, TN, United States
- 96 Petersburg Nuclear Physics Institute, Gatchina, Russia
- 97 Physics Department, Creighton University, Omaha, NE, United States
- 98 Physics department, Faculty of science, University of Zagreb, Zagreb, Croatia
- 99 Physics Department, Panjab University, Chandigarh, India
- 100 Physics Department, University of Cape Town, Cape Town, South Africa
- 101 Physics Department, University of Jammu, Jammu, India
- 102 Physics Department, University of Rajasthan, Jaipur, India
- 103 Physikalisches Institut, Eberhard Karls Universität Tübingen, Tübingen, Germany
- 104 Physikalisches Institut, Ruprecht-Karls-Universität Heidelberg, Heidelberg, Germany
- 105 Physik Department, Technische Universität München, Munich, Germany
- 106 Research Division and ExtreMe Matter Institute EMMI, GSI Helmholtzzentrum für Schwerionenforschung GmbH, Darmstadt, Germany
- 107 Rudjer Bošković Institute, Zagreb, Croatia
- 108 Russian Federal Nuclear Center (VNIIEF), Sarov, Russia
- 109 Saha Institute of Nuclear Physics, Kolkata, India
- 110 School of Physics and Astronomy, University of Birmingham, Birmingham, United Kingdom
- 111 Sección Física, Departamento de Ciencias, Pontificia Universidad Católica del Perú, Lima, Peru
- 112 SSC IHEP of NRC Kurchatov institute, Protvino, Russia
- 113 Stefan Meyer Institut für Subatomare Physik (SMI), Vienna, Austria
- 114 SUBATECH, IMT Atlantique, Université de Nantes, CNRS-IN2P3, Nantes, France
- 115 Suranaree University of Technology, Nakhon Ratchasima, Thailand
- 116 Technical University of Košice, Košice, Slovakia
- 117 Technical University of Split FESB, Split, Croatia
- 118 The Henryk Niewodniczanski Institute of Nuclear Physics, Polish Academy of Sciences, Cracow, Poland
- 119 The University of Texas at Austin, Physics Department, Austin, TX, United States
- 120 Universidad Autónoma de Sinaloa, Culiacán, Mexico
- 121 Universidade de São Paulo (USP), São Paulo, Brazil
- 122 Universidade Estadual de Campinas (UNICAMP), Campinas, Brazil
- 123 Universidade Federal do ABC, Santo Andre, Brazil
- 124 University of Houston, Houston, TX, United States
- 125 University of Jyväskylä, Jyväskylä, Finland
- 126 University of Liverpool, Liverpool, United Kingdom
- 127 University of Tennessee, Knoxville, TN, United States
- 128 University of the Witwatersrand, Johannesburg, South Africa
- 129 University of Tokyo, Tokyo, Japan
- 130 University of Tsukuba, Tsukuba, Japan
- 131 Université Clermont Auvergne, CNRS/IN2P3, LPC, Clermont-Ferrand, France
- 132 Université de Lyon, Université Lyon 1, CNRS/IN2P3, IPN-Lyon, Villeurbanne, Lyon, France
- 133 Université de Strasbourg, CNRS, IPHC UMR 7178, F-67000 Strasbourg, France
- 134 Università degli Studi di Pavia, Pavia, Italy
- 135 Università di Brescia, Brescia, Italy
- 136 V. Fock Institute for Physics, St. Petersburg State University, St. Petersburg, Russia
- 137 Variable Energy Cyclotron Centre, Kolkata, India
- 138 Warsaw University of Technology, Warsaw, Poland
- 139 Wayne State University, Detroit, MI, United States
- 140 Wigner Research Centre for Physics, Hungarian Academy of Sciences, Budapest, Hungary
- 141 Yale University, New Haven, CT, United States
- 142 Yonsei University, Seoul, Republic of Korea
- 143 Zentrum für Technologietransfer und Telekommunikation (ZTT), Fachhochschule Worms, Worms, Germany

i Deceased.

ii Dipartimento DET del Politecnico di Torino, Turin, Italy.

iii M.V. Lomonosov Moscow State University, D.V. Skobeltsyn Institute of Nuclear Physics, Moscow, Russia.

iv Department of Applied Physics, Aligarh Muslim University, Aligarh, India.

v Institute of Theoretical Physics, University of Wrocław, Poland.